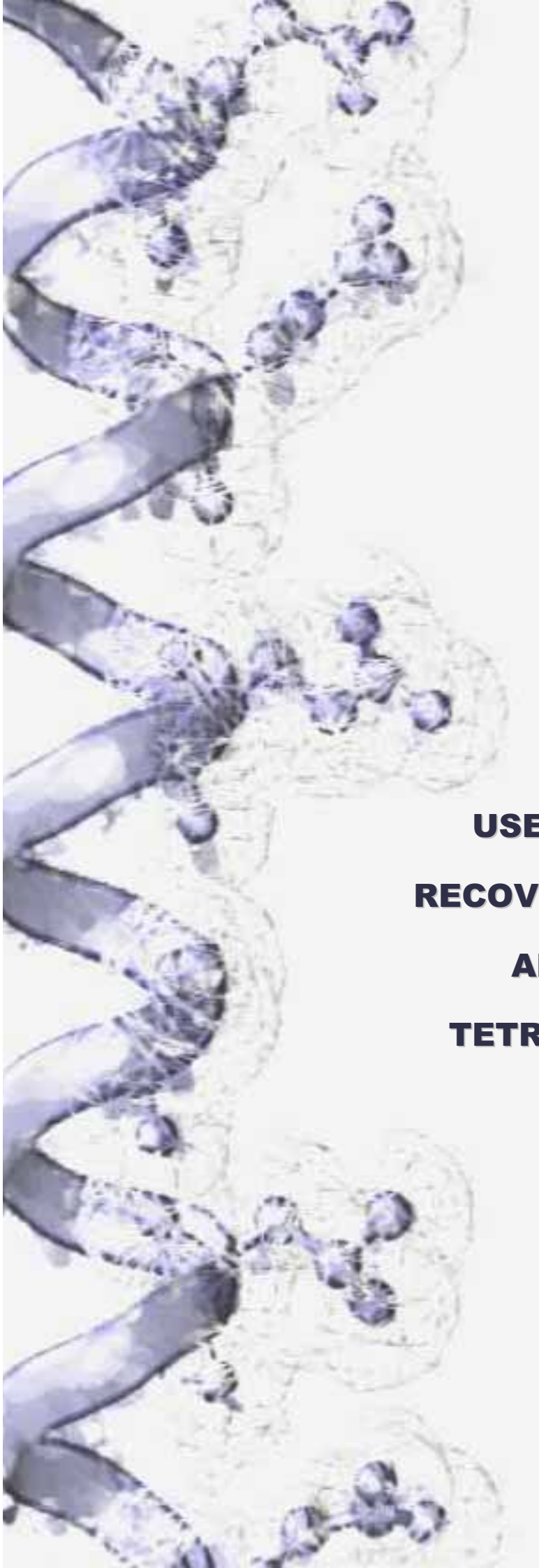

USE OF CALIX[4]ARENES TO RECOVER THE SELF-ASSEMBLY ABILITY OF MUTATED p53 TETRAMERIZATION DOMAINS

Susana Gordo Villoslada

2008

Memòria presentada per

Susana Gordo Villoslada

per optar al grau de doctor per la Universitat de Barcelona

Revisada per:

Prof. Ernest Giralt i Lledó

Universitat de Barcelona

Director

Programa de Química Orgànica

Bienni 2003-2005

Barcelona, abril de 2008

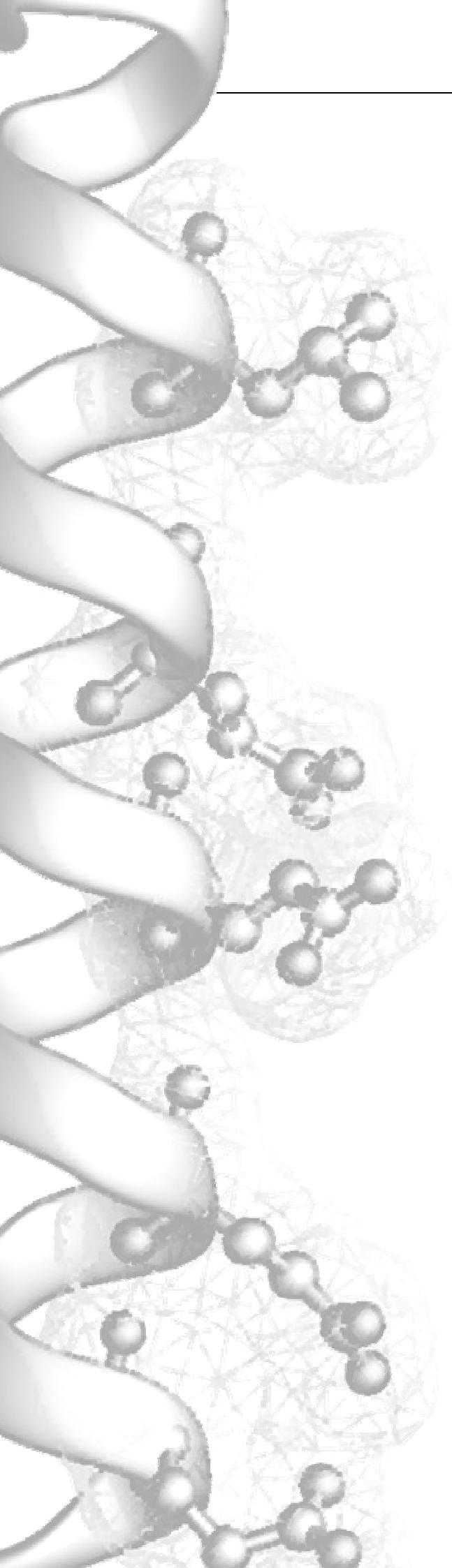

RESULTS

RESULTS 3

Calix4prop: an unexpected ligand for the p53 tetramerization domain

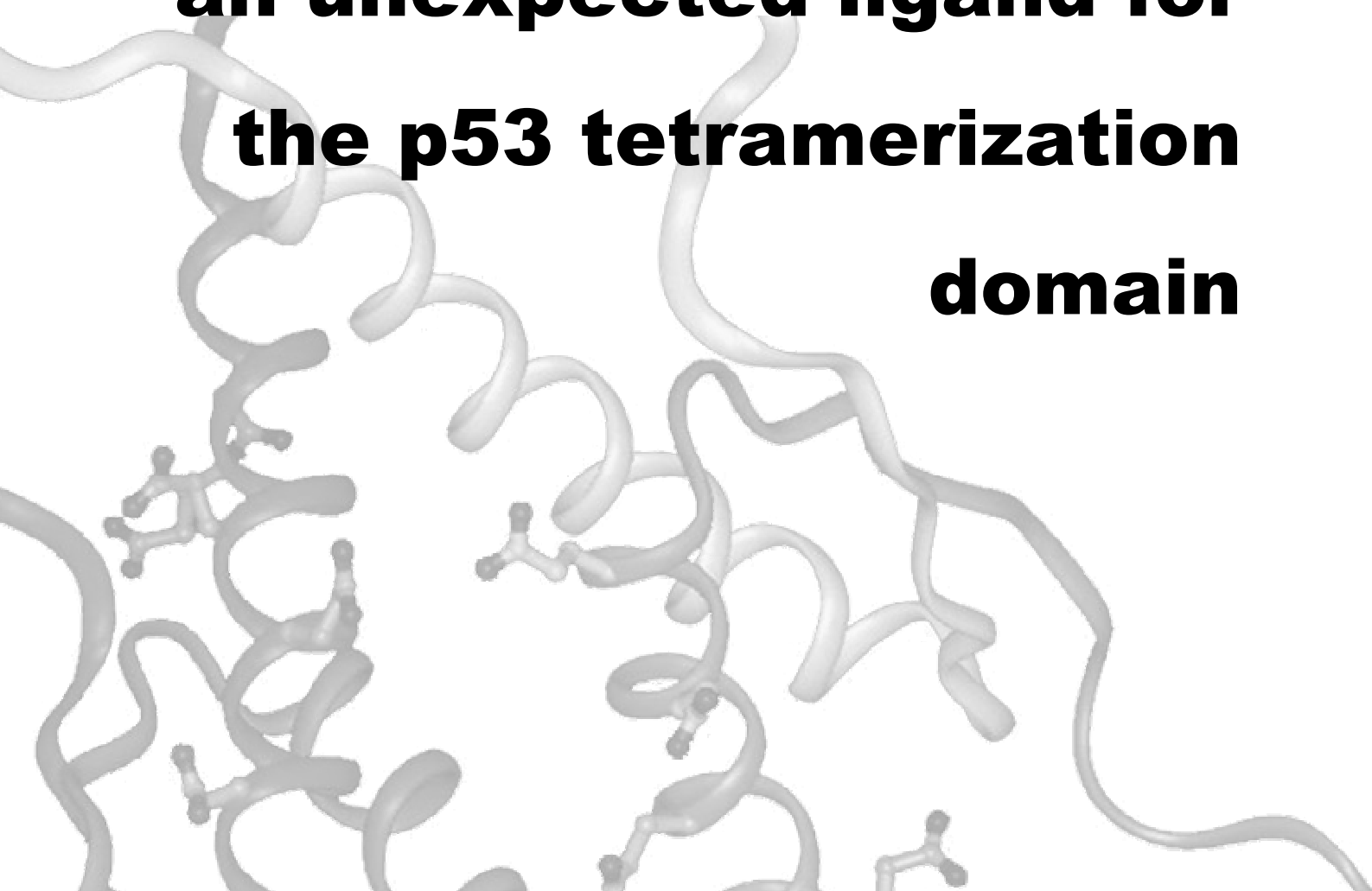

3.1. Calix4prop: the origins

Experimental evidences proved that calix4bridge interacted with the tetrameric p53TD just as it was designed to. The binding of two calixarene molecules thermodynamically stabilized the tetramer assembly for p53TD mutants with compromised tetramerization abilities.

In the design of calix4bridge, neighboring positions of the lower-rim were bridged by a biscrown loop so that the calix[4]arene was made as rigid as possible in order to avoid an additional source of entropic penalty from the binding to the protein pocket.[1] However, had the calixarene ligand been a more flexible structure, what would have happened? Would ligand entropy penalties have precluded the complex formation? Could the entropic loss from the ligand fitting count that much? Or would the interaction of hydrophobic surfaces and ion pairing balance all the negative factors by promoting favorable entropic water rearrangements and strong enthalpic terms?[2]

Moreover, R337H interacted tighter with the calixarene ligand than the well-packed and stable wild-type tetramer. This was ascribed to the flexibility of the mutant protein. Hence, would a more flexible calixarene also result in a tighter interaction?

To answer these questions and gain insights into the relevance of the entropic effect in protein-ligand interactions, a more flexible calix[4]arene ligand was designed: 5,11,17,23-tetraguanidino-methyl-25,26-27,28-propoxycalix[4]arene, named **calix4prop**, for short. This new ligand also was functionalized with four methylguanidinium groups in the upper rim, but its lower-rim consisted of four propyl chains, which were big enough to prevent calixarene internal rotation –and thereby mantain the conical shape– but free enough as not to firmly fix the calixarene conformation.

It must be admitted that, when the ligand was initially designed, it was truly thought that the entropic penalties for ordering the calixarene propyl chains in the lower rim would prevent their fitting into the protein pocket, so that calix4prop would actually serve as a negative control.

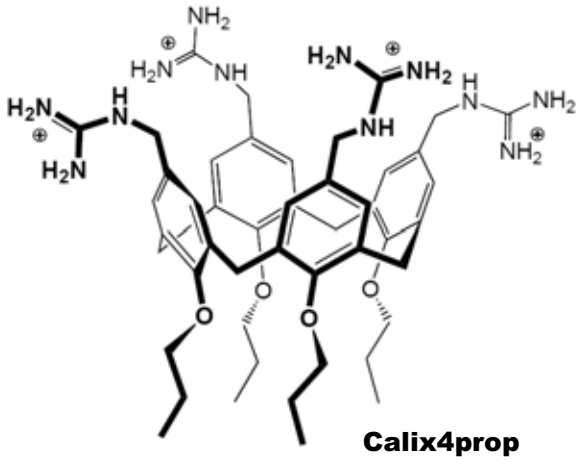

Calix4prop

Nevertheless, experiments revealed an unexpected behavior which had little to do with acting as a negative control. Evaluation of the amino-version of the ligand –**NH_2-calix4prop**– and other calix[4]propyl derivatives helped to better understand the events that take place between calix4prop and p53TD.

3.2. Differential Scanning Calorimentry

The first unexpected result came from the significant thermal stabilization that proteins p53wt and R337H underwent in the presence of calix4prop.

(a) Protein p53wt

The shift towards higher melting temperatures induced by calix4prop on the unfolding of wild-type p53TD was moderate (*i.e.* <4ºC) but the enthalpy of the transition peak from the DSC endotherm increased considerably,[3,4] as can be clearly appreciated in **Figure 3.1A**. Changes in the thermogram were not smoothly progressive with the ligand concentration, which could be the result of an inaccurate trace of the baseline in the raw data.[5] Nonetheless, the endotherm for the sample with the highest ligand ratio was found to be reproducible, and it could fit the mathematical model for the dissociation coupled to unfolding of a tetrameric assembly[6] (Supplementary Material).

The increase in thermal stability was evidently due to the interaction –likely specific– of the tetrameric protein with the ligand, although the origin of the increase in the unfolding enthalpy could not be unequivocally attributed. The additional enthalpy could be the result of a high protein-ligand binding enthalpy.[7] Alternatively, the ligand might have promoted a new protein structure which was more stable than the native one. Regrettably, the current data was not sufficient for determining the mechanism, although it all appeared that the protein was still tetrameric and that its dissociation was coupled to the unfolding, whether the ligand dissociated prior or simultaneously to the protein unfolding.

(b) Mutant R337H

For mutant R337H, the ligand-induced thermal stabilization was impressive, with a final shift in the melting temperature of nearly 30ºC, as shown in **Figure 3.1B**. Actually, the endotherms for the largest ligand ratios were almost the same in both the melting temperature and the unfolding enthalpy, as the corresponding ones for p53wt.

Unfortunately, most of the thermograms for R337H in the presence of calix4prop presented a minor exothermic event at the end of the transition peak that disturbed the endotherm and made complicated tracing of a reliable baseline. Minima in DSC curves are usually associated with aggregation of the unfolded species;[8,9] in this case, aggregation did not seem to be a ligand-dependent event, since not all samples containing ligand displayed it, and no clear trend between the ligand concentration and the magnitude of the exothermic peak was observed.

The inappropriate baseline tracing precluded the fine analysis of the experimental data,[10] and it also was the most likely reason for some variable shifts detected in the transition peaks (**Figure 3.2B**). In any case, it was evident that a new transition peak for the ligand-bound species emerged at higher temperatures, while the former peak from the free protein unfolding disappeared.

Since biphasity is only detected under sub-saturating conditions,[11,12] for the system R337H-calix4prop, at 25μM of tetrameric protein, saturation was reached in the presence of a ligand concentration of *ca.* 65-75μM (at the melting temperature). This provided a good idea of the high affinity that calix4prop displayed for R337H (i.e. a thermodynamic dissociation constant in the sub-micromolar range), which is likely larger than for p53wt (at the melting temperature).[12] The high affinity of the calixarene ligand for R337H could also be one of the reasons for the huge increase in the unfolding enthalpy.

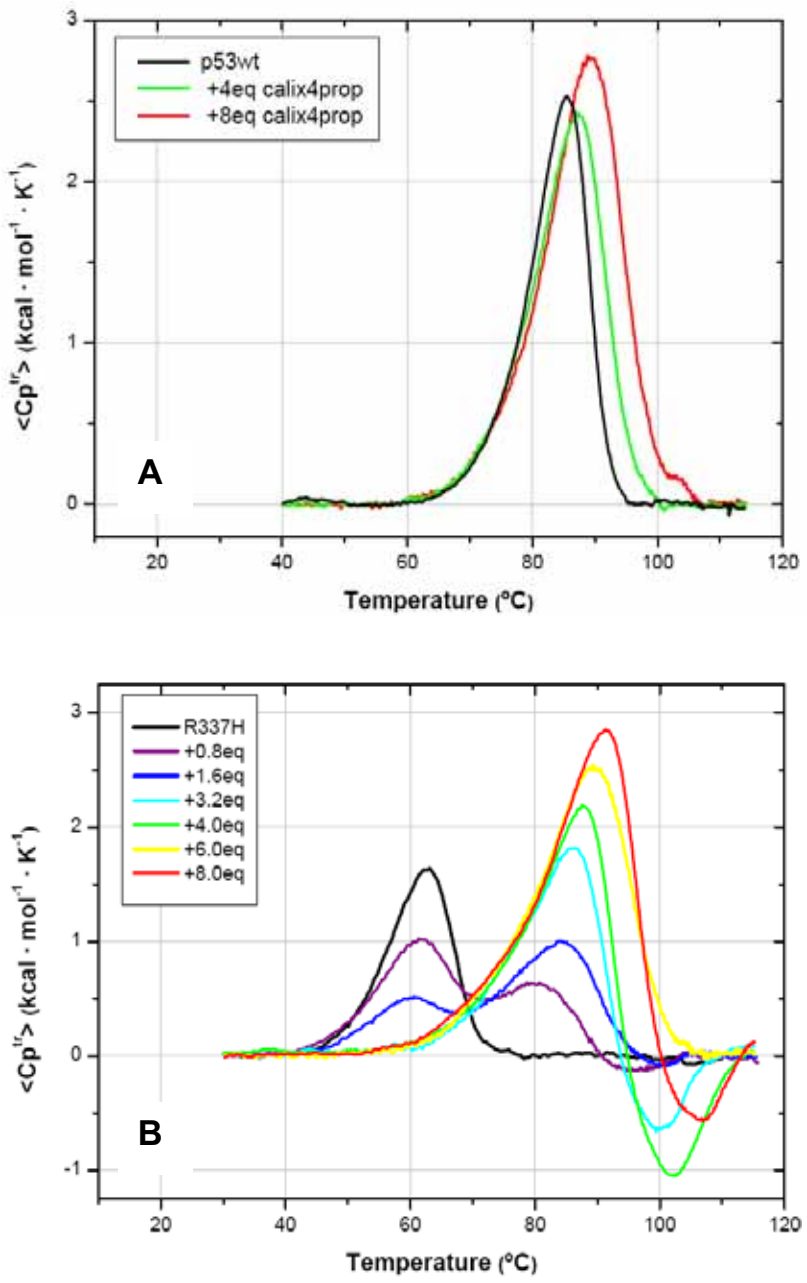

Figure 3.1. DSC thermograms of **(A)** p53wt and **(B)** R337H free (black trace) and in the presence of increasing amounts of calix4prop (molar ratios of ligand relative to 25μM tetramer), in water at pH 7.0.

It is worth noting that the new transition peak for the ligand-bound protein displayed a certain asymmetry –skewed to the lower temperatures– which resembled that of a tetrameric assembly with unfolding coupled to dissociation. Indeed, the only curve without the aggregation contamination (*i.e.* the neat yellow trace in **Figure 3.1**, corresponding to 25μM of tetramer with 150μM of ligand) could fit reasonably well the dissociation-unfolding model described for p53wt[6] (Supplementary Material). Hence, the change in the protein unfolding profile suggested that the ligand was binding to and stabilizing the tetrameric assembly. However, it could not be determined whether the ligand was dissociating form the protein before or during the unfolding. Likewise, the increase in the enthalpy could be either due to the protein-ligand binding or to a different, more stable, protein structure induced by the ligand.

Moreover, given the dependence between the protonated state of H337 and the protein stability, the interaction with calix4prop could also favor the protonation of the histidine side-chain, which would also contribute to stabilize the tetramer.

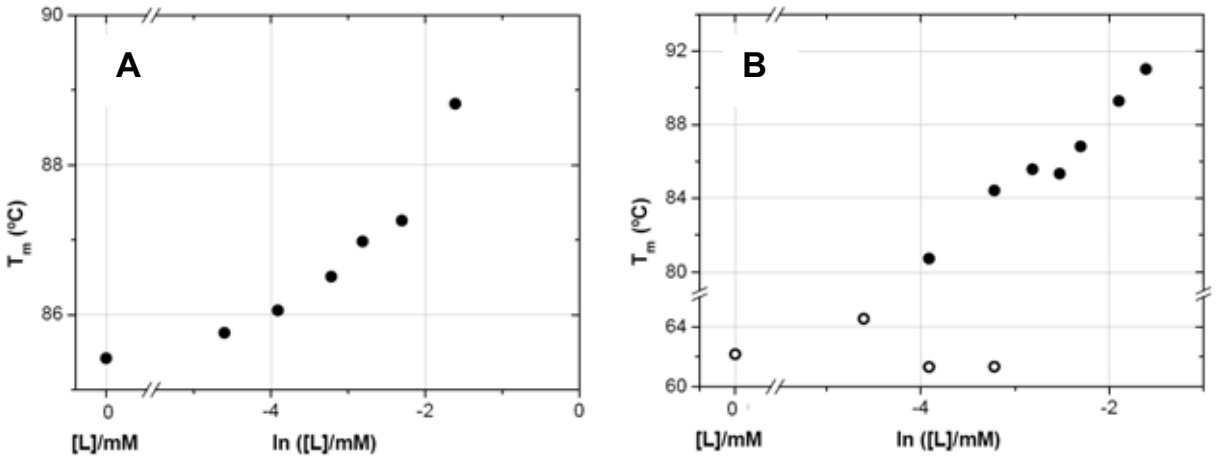

Figure 3.2. Temperatures of the maxima C_P in the DSC transition peaks plotted against the logarithm of calix4prop concentration[13] of **(A)** p53wt and **(B)** R337H. In **(B)**, the solid black dots correspond to the maxima of the transition peak of the ligand-bound species; whereas the open dots represent the melting temperature of the free protein transition peak. Large variations in these data are likely due to inaccuracies in the traced baseline.

3.3. Circular Dichroism

The effects of calix4prop on both the thermal stability and the structure of the proteins also were studied by circular dichroism.

(a) Protein p53wt

The CD spectra for p53wt in the presence of calix4prop did not markedly differ from the free protein one (**Figure 3.3A**). Accordingly to the DSC results, a tiny thermal stability induced by the calixarene also was detected in the CD unfolding profiles (**Figure 3.3B**), although the high noise of the signal made these data fairly inaccurate. The reproduction of the DSC results by CD, despite working at different concentrations (25μM in DSC vs. 2.5μM in CD), clearly indicated that the interaction was specific.

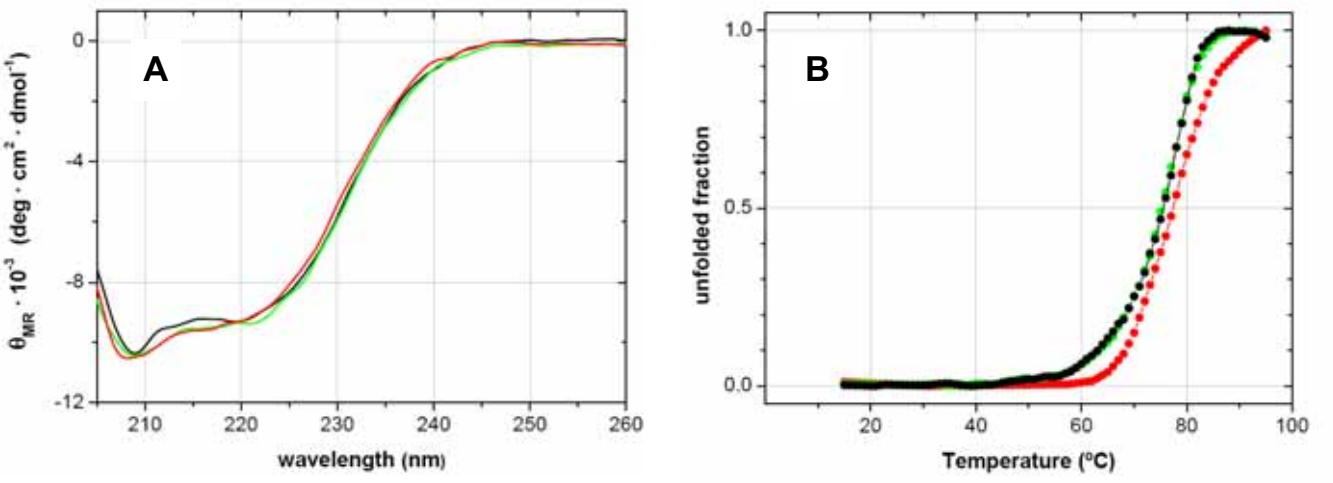

Figure 3.3. (A) CD spectra at 20ºC (7.5μM tetramer) and **(B)** CD melting curves (2.5μM tetramer, θ at 220nm) of p53wt free (black) and in the presence of 4eq (green) and 8eq (red) of calix4prop (molar ratios relative to tetramer), in water at pH 7.0. Samples with the highest ligand ratio are fairly inaccurate due to the high noise level in the raw data.

(b) Mutant R337H

CD changes for R337H in the presence of calix4prop were more evident, in both the secondary structure and the unfolding profile. As expected from the DSC results, the CD unfolding curves (**Figure 3.4**) were largely shifted towards higher temperatures (ΔT_{05} ~25ºC). Interestingly, the unfolding profile for R337H and p53wt in the presence of 8 equivalents of ligand were very similar, just as observed by DSC (**Table 3.1**).

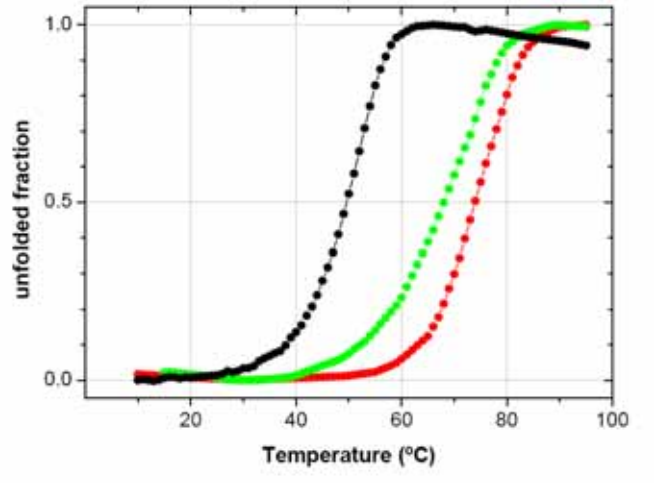

Figure 3.4. CD melting curves of R337H, free (black) and in the presence of a 4eq (green) and 8eq (red) of calix4prop (relative to 2.5μM tetramer), monitoring ellipticity at 220nm; in water at pH 7.0.

The interaction of R337H with calix4prop induced significant changes in the CD spectrum (**Figure 3.5**). Despite the thermal stabilization promoted by the ligand, the protein seemed to "lose" secondary structure, or at least, the CD minima at 208 and at 222nm (from the α-helix) lost intensity. The decrease occurred in conjunction with a suspicious shift in the slope at approximately 240nm. The most plausible explanation for said decrease would be the loss of secondary structure; however, another possibility is that in the binding event, aromatic moieties from the protein and/or from the ligand were affected such that their UV absorption arose in that region.[14-17]

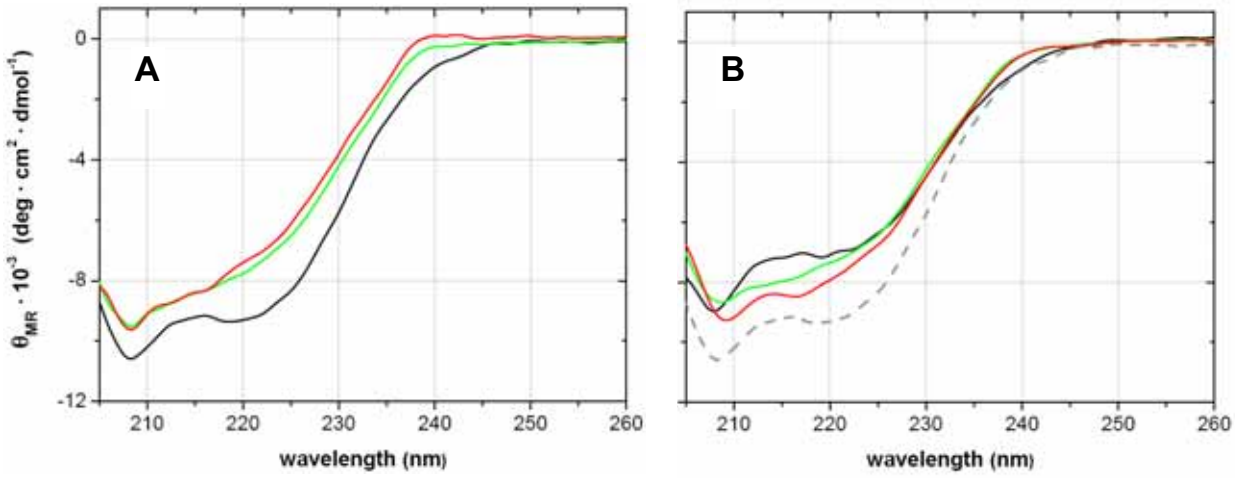

Figure 3.5. CD spectra **(A)** at 20ºC and **(B)** at 55ºC of 7.5μM (tetramer) R337H, free (black solid line) and in the presence of 4eq (green) and 8eq (red) of calix4prop (relative to tetramer). The dotted grey line in **(B)** corresponds to the free protein at 20ºC. All traces in water at pH 7.0.

Alternatively, the decrease in the CD ellipticity could be attributed to the disruption of the α-helix bundle of the tetramer. It is known that when α-helices interact with themselves, the minimum at 222nm increases with respect to that at 208nm[a].[18] For R337H, the presence of calix4prop promoted the opposite, which could be interpreted as a disruption in the helix bundle by the ligand. This would not necessarily imply a loss of secondary structure or of tetramerization, but the interaction with the ligand would certainly affect the structure of the whole protein.

Table 3.1. Thermal stabilization by calix4bridge (T_{05} in ºC)

	T_{05} DSC*			T_{05} CD**		
	P	**+4eq L**	**+8eq L**	**P**	**+4eq L**	**+8eq L**
p53wt	84	87.7	88.7	75.5	75.5	77.5
R337H	61.5	87	~89	49.5	68	77

* 100μM monomer; T_{05}: at which ½ ΔH_m.

** 10μM monomer; T_{05}: at which the f_u is ½

(c) Mutant G334V

The behavior of the mutant G334V strongly differed from those of the other proteins. At room temperature, the CD spectrum in the presence of calix4prop did not differ from that of the free protein (**Figure 3.6A**), but that changed at higher temperatures. If the free protein was heated at 55ºC for a while, it underwent some unfolding –just as would be expected for a protein whose melting temperature is *ca.* 65ºC. However, if calix4prop was present, G334V underwent a puzzling structural transformation which was slow –or fast– enough as to be followed by recording successive CD spectra, as shown in **Figure 3.6C** and **D**. The structural rearrangement induced by calix4bridge was far from a simple unfolding process; in fact, it resembled a β-transformation,[19] although the final spectra did not present the typical minimum at 210nm for β-sheets.[b] It seemed to present a maximum at 195nm, but the high voltage of the signal at these low wavelengths (*ca.* 700V) make the data somewhat questionable.

The structural rearrangements induced by calix4prop were completed after 30 minutes, and the greater the amount of calixarene, the faster the rearrangement (**Figure 3.6C** vs. **D**). Interestingly, when samples were cooled back at room temperature (**Figure 3.6E**), the protein experienced another structural transformation, which had little to do with the previous one. The CD spectrum for that new conformation displayed a wide minimum about 200nm, and the maximum at 195nm had completely vanished. The amount of calixarene also conditioned the rate of this second change (**Figure 3.6E**) but, once formed, it was a highly stable structure and lasted for several days (**Figure 3.6F**).

[a] **Parameter *q*** = $\theta_{220}/\theta_{208}$; q <1 for single stranded α-helix and q ≥1 for interacting helices.

[b] CD profiles for β-sheets are variable, and the minimum at 210 nm is by no means a universal feature.[19]

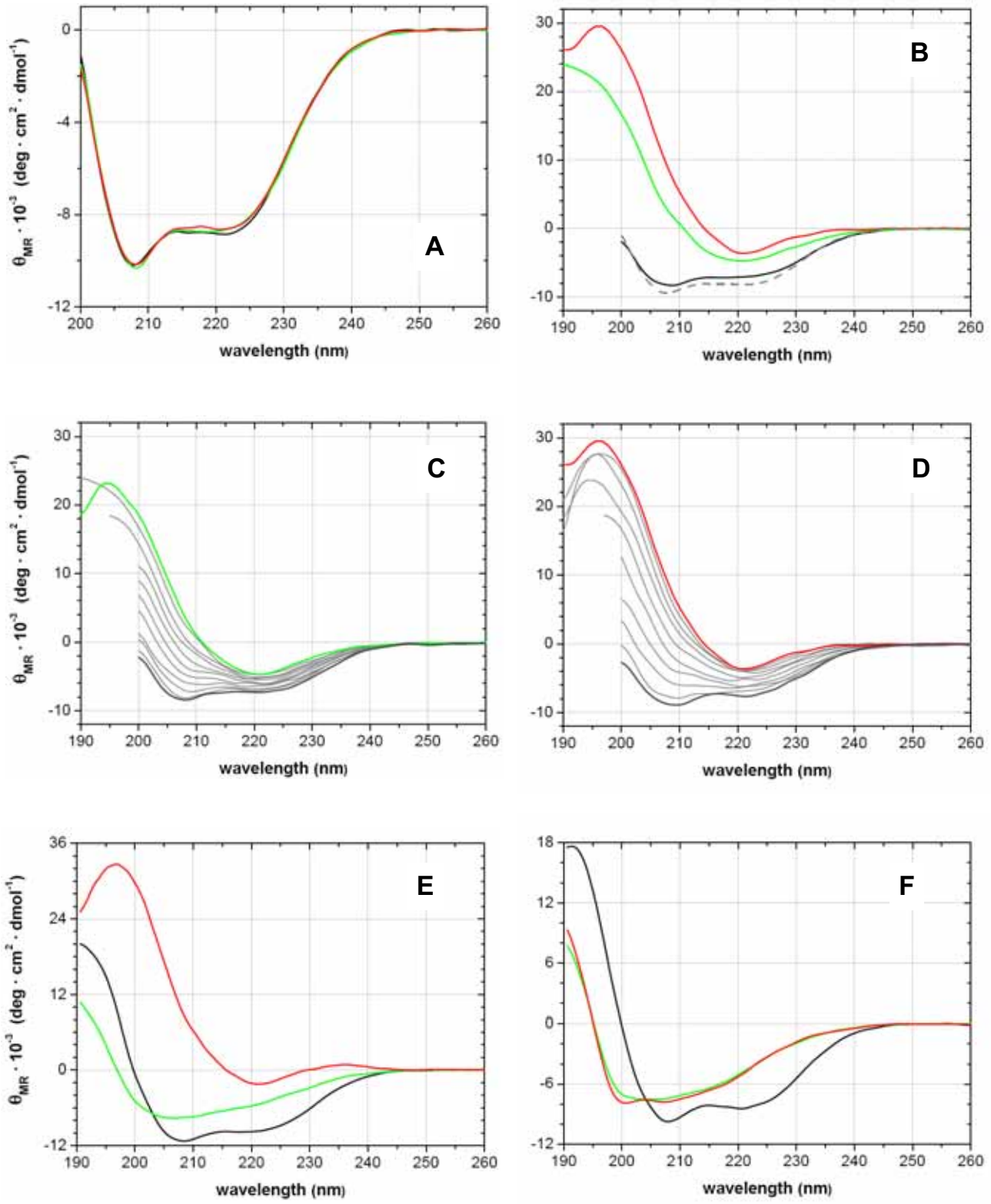

Figure 3.6. CD spectra **(A)** at 20ºC and **(B)** after 30min at 55ºC of 7.5µM (tetramer) G334V, free (black solid line) and in the presence of 4eq (green) and 8eq (red) of calix4prop. The dotted grey line in **(B)** corresponds to the free protein at 20ºC. The progressive structural transformation taking place at 55ºC is displayed in **(C)** for the 4eq and **(D)** for the 8eq samples. The first scan is shown in dark grey, and the successively recorded spectra (3min each) are shown in light grey. **(E)** CD spectra of the samples **C** and **D** just after cooling at 20ºC and **(F)** after 1 day. In water at pH 7.0

That same CD final profiles shown in **Figure 3.6F** have been described for some amyloidal aggregates of the Aβ(1-40).[20-22] Contrariwise, these spectra did not resemble those reported for β-aggregates of the recombinant R337H[23] or the synthetic G334V[24] tetramerization domains, both of which exhibit the typical minimum at 210nm.

Melting curves for G334V protein in the presence of calix4prop –when heating is continuous and faster– were not shifted towards higher temperatures, as would be expected from the stabilizing effects observed in the other proteins. In fact, the unfolding trace appeared equivalent to that for the free protein (**Figure 3.7A**), although the CD spectrum of the denatured protein clearly showed that the β-rearrangement had occurred (**Figure 3.7B**).

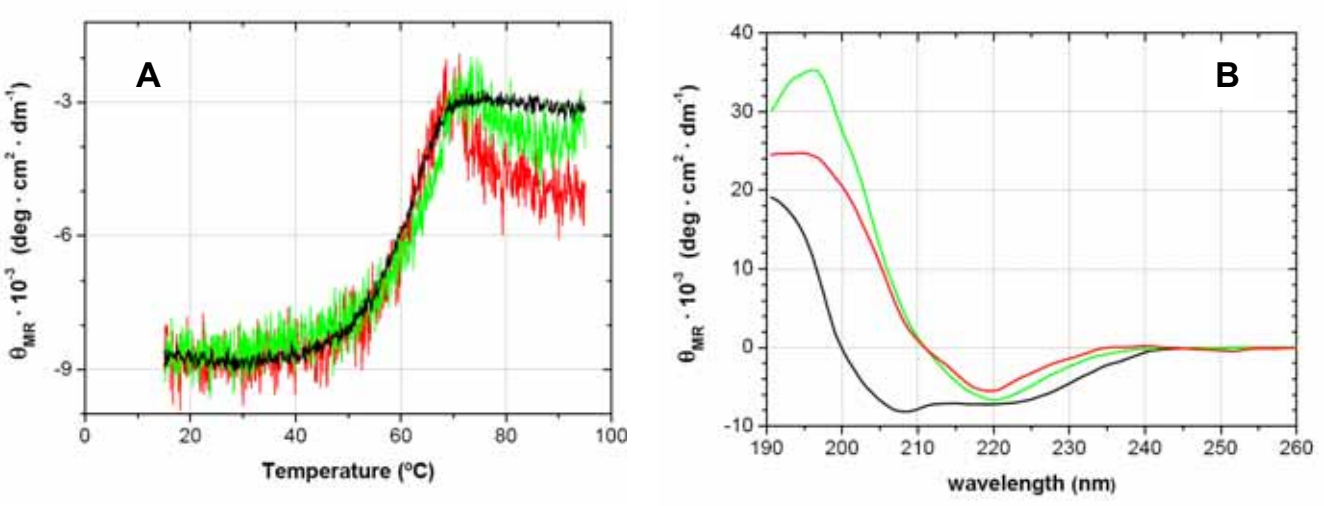

Figure 3.7. (A) CD melting curves of G334V free (black) and in the presence of 4eq (green) and 8eq (red) of calix4prop (relative to 2.5μM tetramer), heating at 90ºC/h, following ellipticity at 220nm. Raw data is directly display to better appreciate the changes. **(B)** CD spectra at 20ºC of the denatured samples from **(A)**. In water at pH 7.0.

The aforementioned observations led to the conclusion that calix4prop promoted (or accelerated) the β-amyloidogenesis in mutant G334V. Heating helped the structural transformation, which could suggest that the protein probably first needed to lose its native structure before undergoing conformational rearrangement. The role of calix4prop in this process remains unknown.

The question which then arises is whether this phenomenon is peculiar to G334V or could occur in other proteins. Experiments on the wild-type tetramerization domain and mutant R337H did not show so. Indeed, calix4prop stabilized the tetrameric assembly for both proteins, although some unidentified changes were induced on R337H structure. Perhaps, it would be a matter of time rather than temperature to also observe calix4prop-induced amyloidogenesis for those proteins.

As a negative control, the CD spectrum of mutant L344P in the presence of calix4prop was also recorded. Nothing was detected at either room temperature, or 55ºC, or longer incubation times (see Supplementary Material).

3.4. NMR structural characterization

The large thermal stabilization of p53wt and R337H in the presence of calix4prop was direct evidence of the strong interaction between each of these proteins and the ligand. However, how was the molecular recognition of these occurring (at low temperatures)? This issue was addressed from a structural perspective using NMR.

3.4.1. NMR on the protein

3.4.1.1. Chemical shift perturbation by ^{15}N-^{1}H-HSQC

In order to determine which parts of the protein structure were involved in the interaction with calix4prop, a titration of ^{15}N-protein with increasing amounts of ligand was followed by ^{15}N-^{1}H-HSQC, in water at pH 7 and at 25ºC. Calix4prop was added to the protein until no more changes were detected in the protein spectra or until species precipitated.

(a) Protein p53wt

The overlapped spectra for the titration of protein p53wt can be found in the Supplementary Material; for clarity, **Figure 3.8** displays the details for some representative residues.

Almost every single protein resonance –from both the backbone and the side-chains– was perturbed by the presence of calix4prop. In general, HSQC peaks experienced a decrease in intensity when the ligand was added, up to completely disappearence at nearly 4 equivalents of ligand (relative to the tetramer). Addition of more calixarene caused the resonances to re-emerge, although generally in a different unidentified location where then they remained and increased in intensity.

The described behavior corresponded to a typical slow chemical exchange process (on the NMR-time scale), thus suggesting a rather large binding affinity.[25] However, it must be noted that slow chemical exchange on the NMR-time scale depends not only on a slow kinetic dissociation constant (k_{off}), but also on the shift difference between the resonances of the free and bound states ($\Delta\delta$). For the present case, some resonances with short shifts (*e.g.* T329, **Figure 3.8**) still displayed the slow exchange behavior, which further suggested a rather slow k_{off}. A slow dissociation also can not be unequivocally correlated with a high affinity association, since the thermodynamic equilibrium constant also depends on the association rate ($K_D=k_{off}/k_{on}$). Nevertheless, the association event is usually limited by the diffusion of the molecules in solution (*ca.* 10^5-10^6 $M^{-1}s^{-1}$),[26] and the approximation is fairly correct.

That almost every residue within the protein was affected suggested that the tight binding of the ligand might induce significant structural rearrangements.[27]

However, changes in the HSQC spectra could not be explained by the occurrence of only a single event. If only one molecule of ligand was tightly bound, the tetramer would lose its symmetry and the number of peaks in the HSQC spectra should be doubled at the end of the titration. Therefore, at least two molecules should bind to a tetramer and thus keep the symmetry of the four monomers. Given that no intermediate was detected, the second binding should be also be in the slow exchange regime and likely of larger affinity than the first one.

The loss of the trace for most of the resonances throughout the titration made the final mapping of protein residues impossible. Mapping the changes in the peak height during the first stage was not helpful, since most of the resonances experienced similar changes. Likewise, the initial decrease in the peak height could not be clearly adjusted to a one-to-one binding model (*i.e.* one ligand binds to one tetramer) because of the inaccuracy of the experimental data and because of the existence of a second binding that shifted the first one. Hence, little could be said about the molecular recognition event, besides the high affinity of the cooperative sequential binding of at least two molecules of calix4prop, and the consequent structural rearrangement that this induced in the protein.[c]

The illustration in **Figure 3.10** represents a possible interaction mechanism. Although the binding sites are actually unknown, considering the hydrophobic nature of the calixarene propyl chains, it could be hypothesized that these might interact with the hydrophobic pocket on the protein surface. Once there, the propyl chains would probably strongly interact with the non-polar environment, which could even affect the highly hydrophobic α-helix bundle in the core of the protein structure. The large structural rearrangements that such interaction would imply –together with the tight interactions anchoring the ligand into the protein– might be the reason for the slow dissociation rate.[32] The binding of the first molecule enhanced the affinity for the second one; therefore, the initial rearrangement should affect the structure of the second binding site. One possibility is that some hydrophobic surface of the protein became solvent exposed; hence, its thermodynamic instability and its easy access would totally shift the equilibrium towards the doubly-bound form.

Better understanding of the binding mechanism for calix4prop and p53wt was attained evaluating the effects of the tetraamino-version of the ligand, called **NH_2-calix4prop**, in which the four guanidinium groups of the upper rim were substituted by amino ones.

The overlapped HSQC spectra for the titration of p53wt with NH_2-calix4prop are provided in the Supplementary Material, and the details for some residues are presented in **Figure 3.9**. The progress of the resonances during the titration was clearly divided into two stages. At the lower ligand ratios, most of the resonances experienced a progressive unidirectional shift that was accompanied by a decrease in the peak height. At 8 equivalents of ligand (relative to tetrameric protein), the resonances had vanished. Further addition of NH_2-calix4prop made the peaks re-emerge elsewhere. The new set of resonances was similar –but not exactly the same– to that

[c] There are formalism for calculation of kinetic constants –and thereby, affinities– from the resonances line shape.[28-31] Such mathematical analysis is not trivial and lies out of the scope of this dissertation.

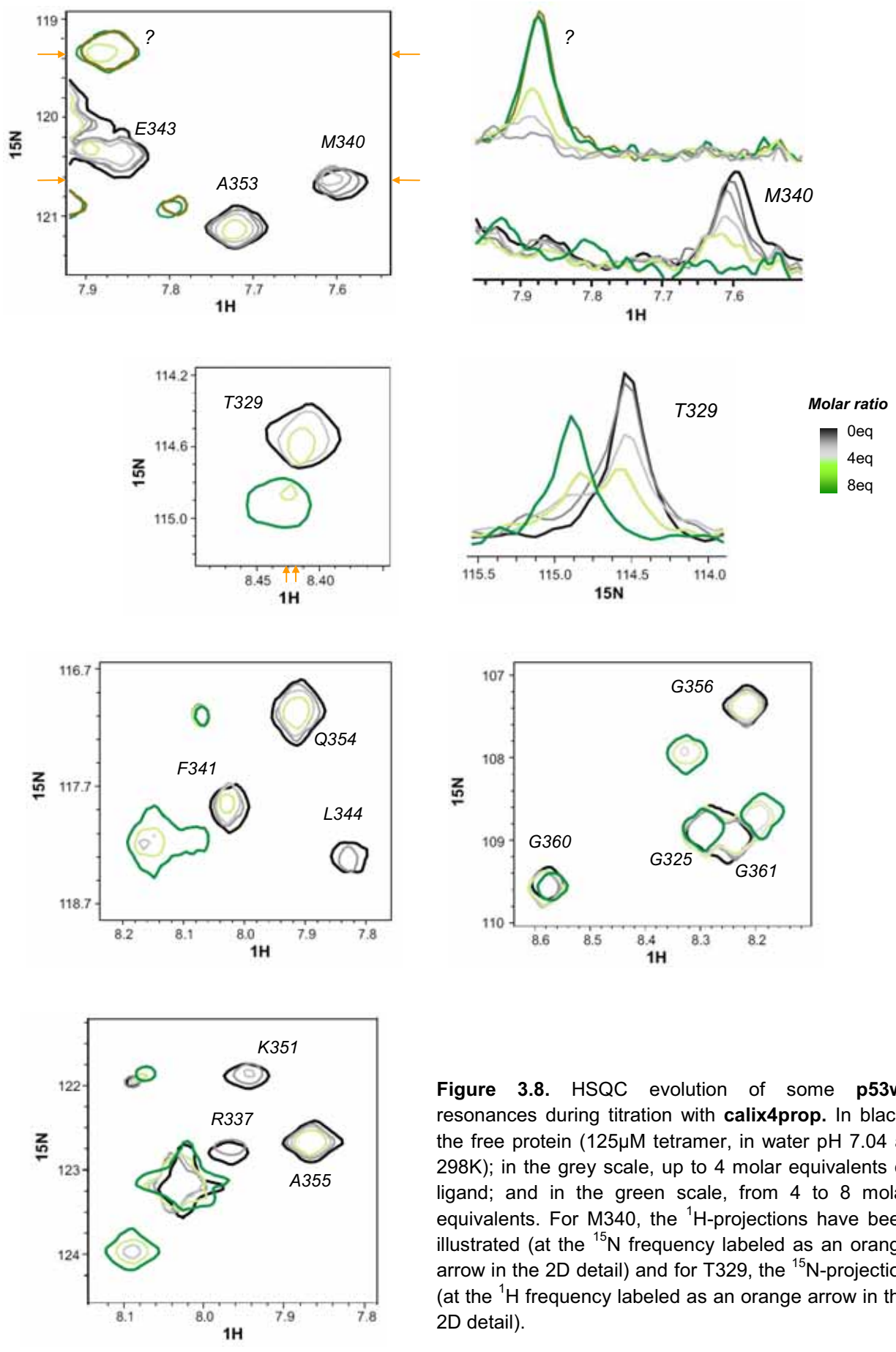

Figure 3.8. HSQC evolution of some **p53wt** resonances during titration with **calix4prop.** In black, the free protein (125μM tetramer, in water pH 7.04 at 298K); in the grey scale, up to 4 molar equivalents of ligand; and in the green scale, from 4 to 8 molar equivalents. For M340, the ^{1}H-projections have been illustrated (at the ^{15}N frequency labeled as an orange arrow in the 2D detail) and for T329, the ^{15}N-projection (at the ^{1}H frequency labeled as an orange arrow in the 2D detail).

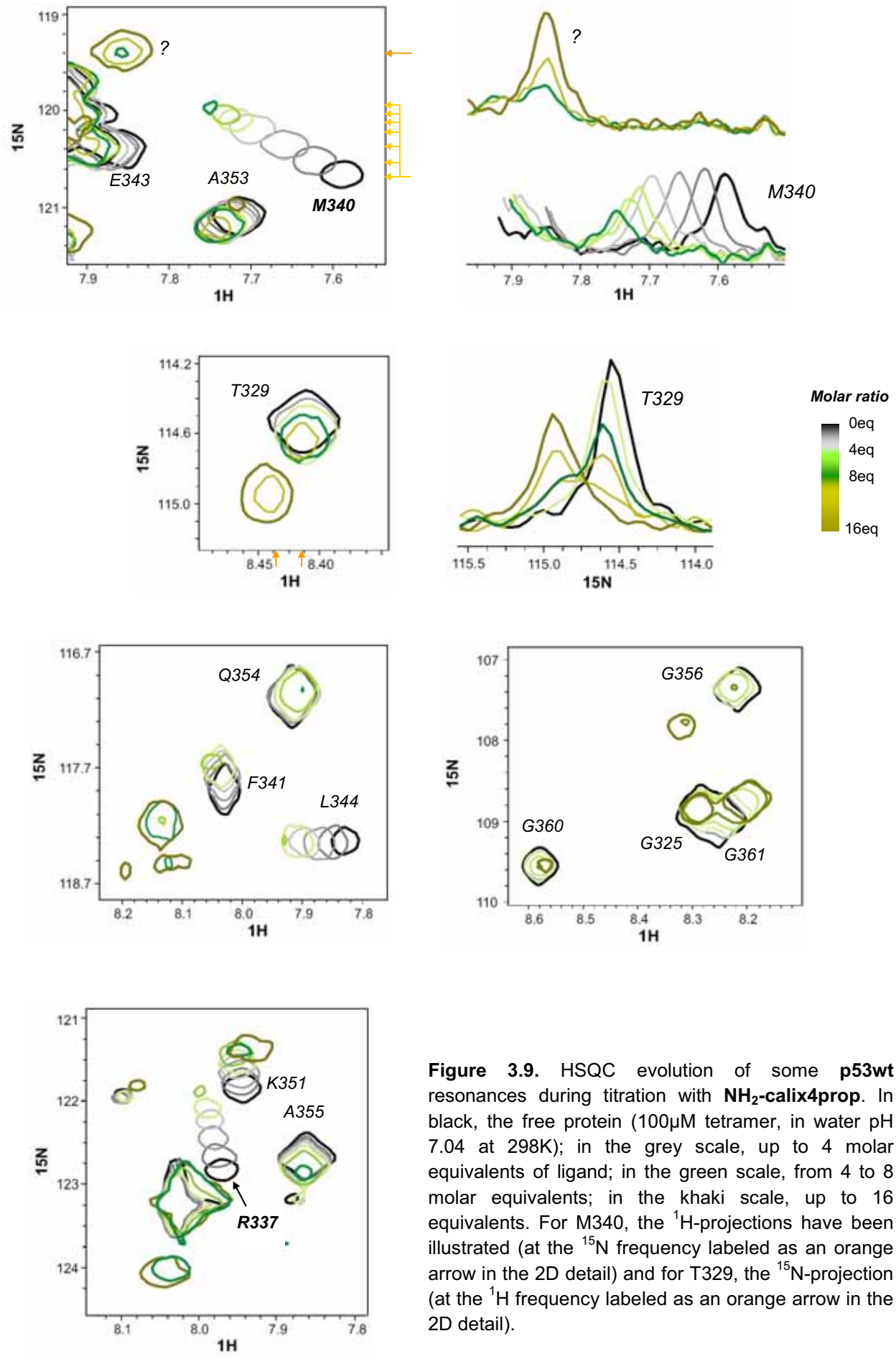

Figure 3.9. HSQC evolution of some **p53wt** resonances during titration with **NH_2-calix4prop**. In black, the free protein (100μM tetramer, in water pH 7.04 at 298K); in the grey scale, up to 4 molar equivalents of ligand; in the green scale, from 4 to 8 molar equivalents; in the khaki scale, up to 16 equivalents. For M340, the ^{1}H-projections have been illustrated (at the ^{15}N frequency labeled as an orange arrow in the 2D detail) and for T329, the ^{15}N-projection (at the ^{1}H frequency labeled as an orange arrow in the 2D detail).

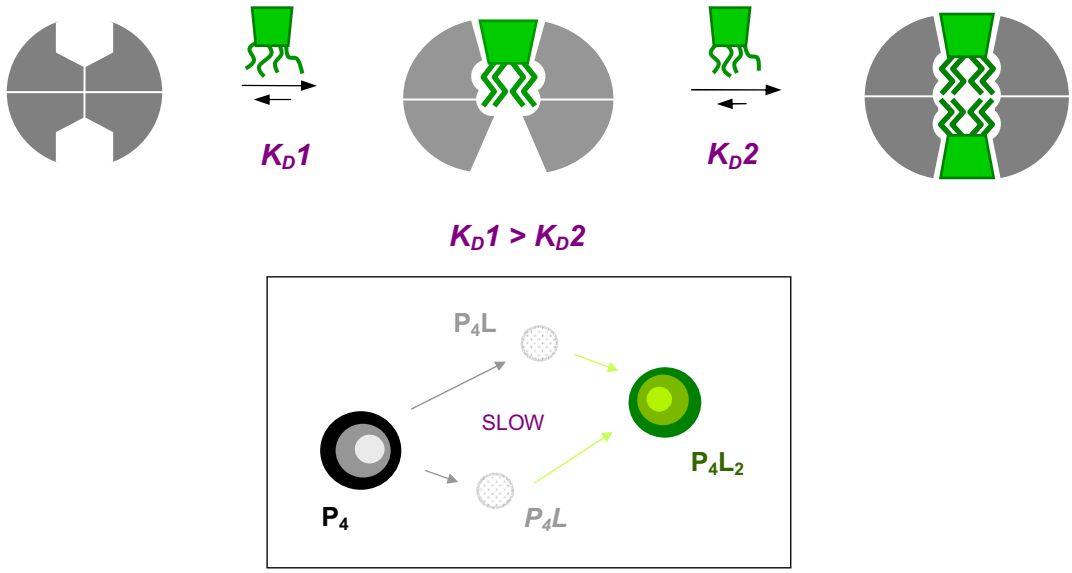

Figure 3.10. Hypothetical sequential binding mechanism of two molecules of **calix4prop** with **p53wt**, and the corresponding evolution for an HSQC resonance. The asymmetric intermediate was not detected because of the positive cooperation of the bindings. Owing to the slow chemical exchange, the protein loses its symmetry in the intermediate; resonances represented as P_4L and P_4L would correspond to the same residue, which is split due to the loss of symmetry upon binding of the first molecule of calix4prop. The binding would probably also fix a preferred conformation in calix4prop.

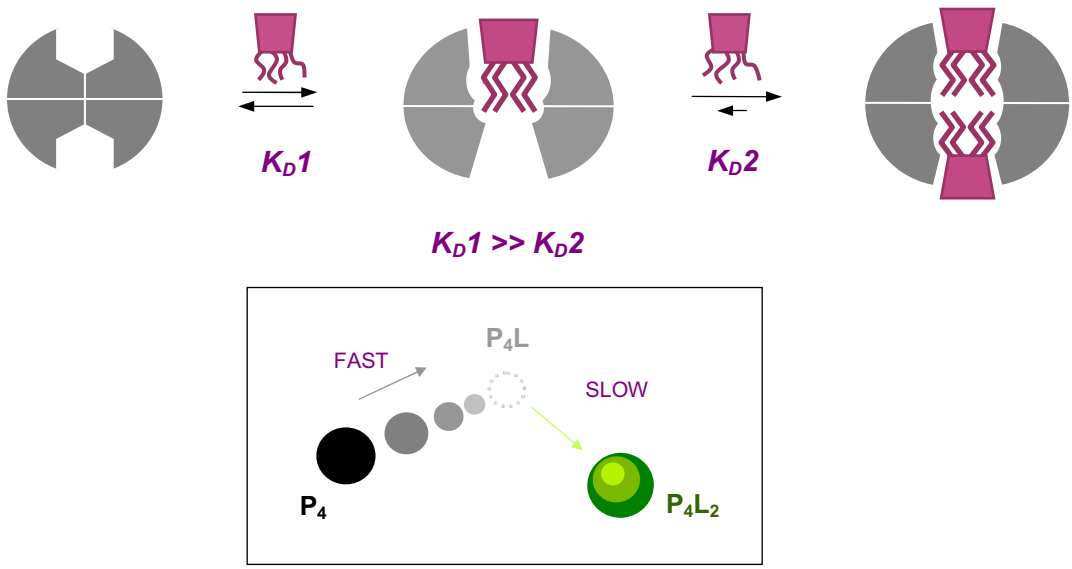

Figure 3.11. Hypothetical sequential binding mechanism of two molecules of **NH_2-calix4prop** with **p53wt**, and the corresponding evolution for an HSQC resonance. This binding also is positively-cooperative, but not as tight as for the tetraguanidinium calix4prop.

detected for the guanidinium-calix4prop. Following the shifting direction of the resonances in the first stage did not always lead to a new peak in the second stage. This observation could be rationalized by a second, higher affinity ligand binding in a slow exchange regime.[32] If this was the case, then the sequential binding of two ligand molecules would again be positively-cooperative.

The affinity for the first binding was roughly approximated from the shifts of the resonances during the first stage (**Figure 3.12**). A dissociation constant of ~300μM resulted from the adjustment of the experimental data to a one-to-one binding model (*i.e.* one ligand binds to one tetramer). This large value was in agreement with the fast chemical exchange, but did not represent the real value, since the second binding event –sequential and of higher affinity– was shifting the first equilibrium.

The large shift experienced by some resonances during that first stage supported the hypothesis that the protein might undergo large structural rearrangement. Moreover, guanidinium groups seemed to be crucial for that rearrangement to take place easily, which would highlight the key role of the ion-chelation in the anchoring of the ligand.

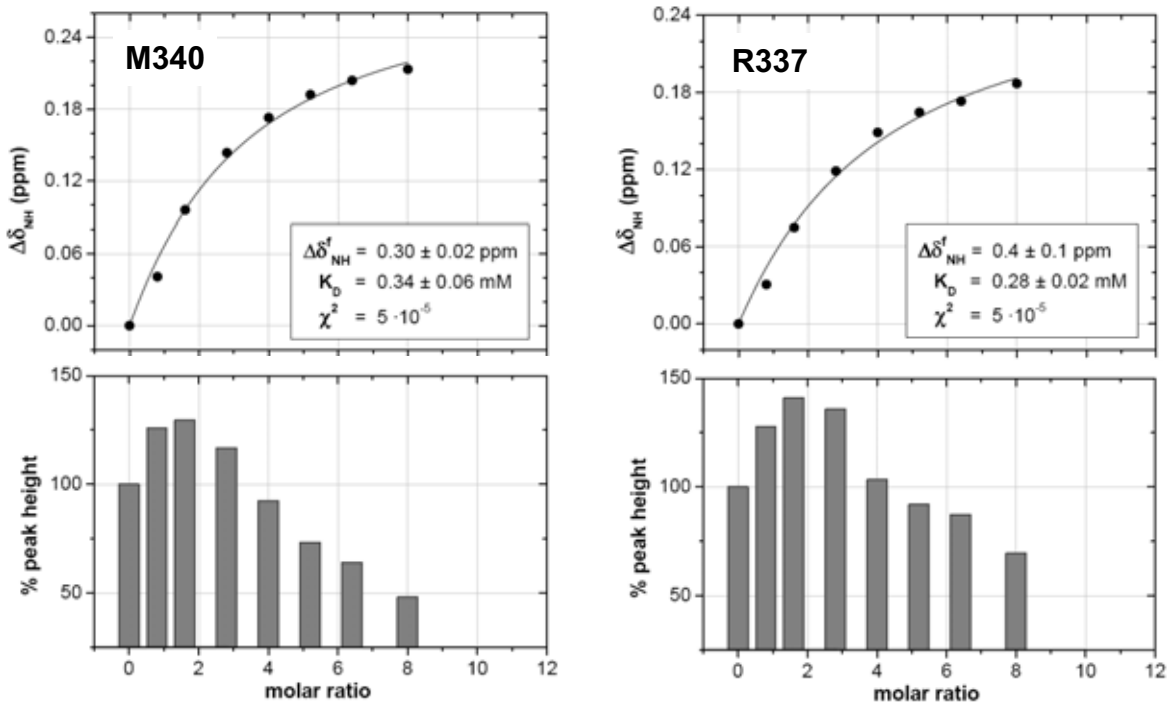

Figure 3.12. Top panels: fitting to a 1:1 model of the unidirectional chemical shift perturbation experienced by resonances M340 and R337 of p53wt along the first stage of NH_2-calix4prop titration. Bottom panels: evolution of the peak height of the above resonances (molar ratios with relative to tetramer).

For NH_2-calix4prop, the residues within the protein that experienced the largest perturbation during the first stage could be mapped (**Figure 3.13**). Representation of the resonances that underwent the greatest shift on the 3D-structure of the protein clearly showed that the most sensitive residues were deep inside the hydrophobic pocket, within the solvent-buried core. This arrangement would

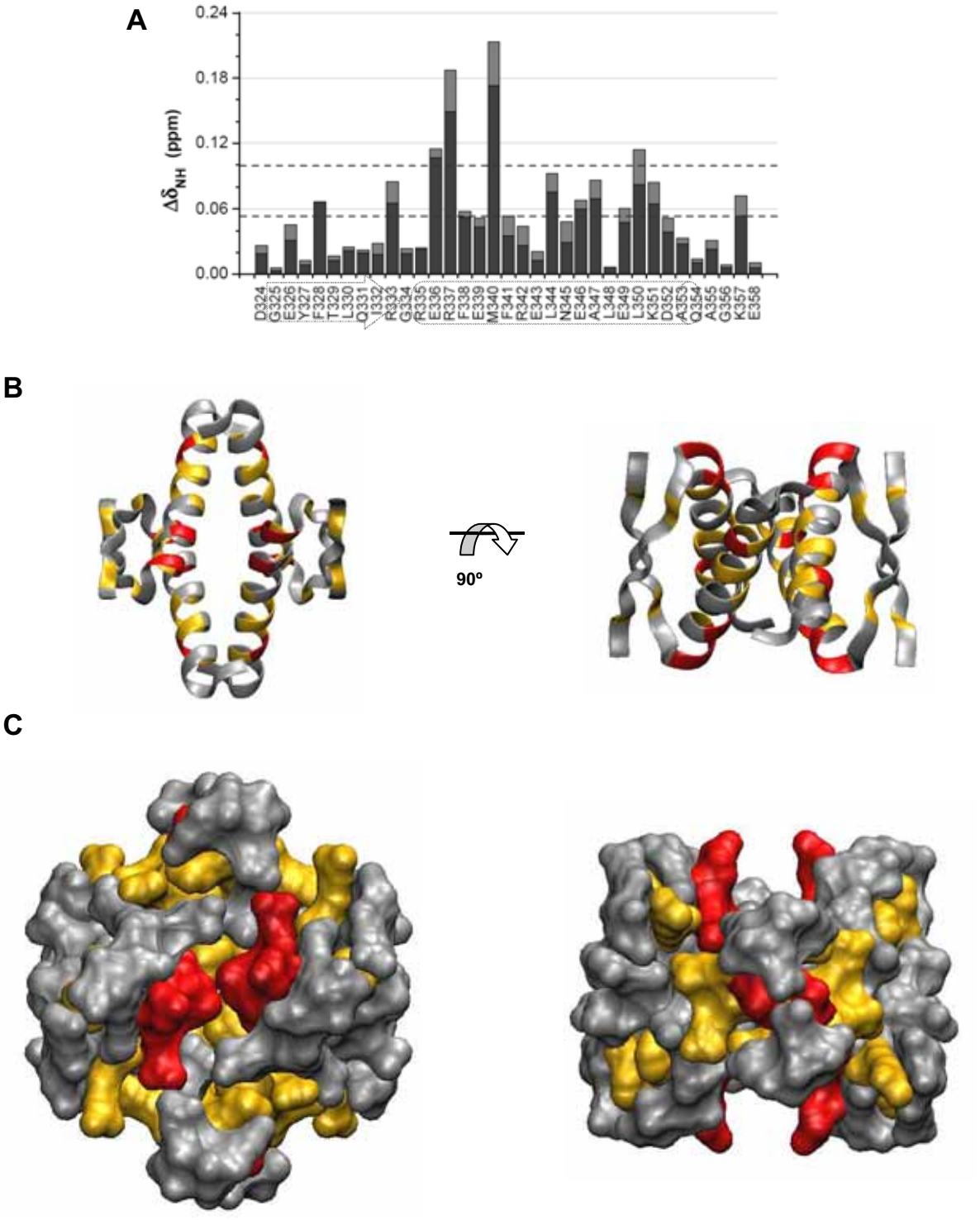

Figure 3.13. p53wt mapping during the first stage of **NH_2-calix4prop** titration. **(A)** Chemical shift mapping at 4eq (dark grey) and 8eq (light grey) of ligand. The dashed lines drawn across represent the cutoff limits used to categorize the degrees of chemical shift for mapping p53TD structure in **(B)** the ribbon and **(C)** the surface diagrams: in red, residues with changes ≥0.1ppm (mean shift plus one standard deviation) and in orange, those changing ≥0.053ppm (the mean shift). The representation at the left shows an upper view of the hydrophobic pocket.

support the hypothesis previously suggested, where the propyl chains would “go deep” into the protein hydrophobic heart. Of course, it could also be possible that the core was perturbed without direct interaction with the ligand; however, if the core had been “opened”, then the former hydrophobic interactions would have been weakened.

(b) Mutant R337H

Was the hypothetic mechanism suggested for wild-type p53TD also suitable for the interaction of calix4prop with the mutant proteins?

The overlapped spectra for the titration of ^{15}N-R337H with calix4prop are provided in the Supplementary Material. Details for some of the resonances are presented in **Figure 3.19**. The changes were very similar to those described for p53wt. At the lowest ligand concentrations, the intensity of protein resonances progressively decreased; they completely disappeared at *ca.* 3-3.5 equivalents of ligand (with respect to 125μM tetramer), a lower ratio than for p53wt. Further ligand addition caused a new set of resonances to emerge, a few which were even shifted when more ligand was added –although this trend was not a general (most of them just remained in position and increased in intensity).

The hypothesis of two molecules sequentially binding to the protein could also explain the changes observed in the R337H spectra. The binding of the first one, likely in a slow exchange regime, might present even higher affinity than for p53wt, since similar changes arose with lesser ligand. The second binding was probably of higher affinity than the first one; otherwise an asymmetric intermediate would have been detected. The final shift for a few of the new resonances –which were small– could correspond to some kind of minor structural rearrangement that only affected a few residues. Unfortunately, the new peaks were mainly unidentified; hence, it was not possible to identify which parts of the protein changed. Considering the tightness of the interaction with the ligand, it could be that those residues in direct contact with the ligand molecule could remain still, while those solvent exposed might be slightly rearranged (**Figure 3.15**).

Of course, the third event could also be attributed to the binding of another molecule of calix4prop, although it is hard to imagine an extra binding site in the structure of the protein-ligand complex.

In conclusion, the binding of two molecules of calix4prop to R337H probably proceeded sequentially and cooperatively, just as hypothesized for p53wt. The ligand displayed higher affinity for the mutant protein than for p53wt. That would also be in line with the suggested mechanism. If the ligand was interacting directly with the buried, hydrophobic core of the protein, then it is logical that the interaction with R337H could be easier: *(i)* for this mutant the tetramerization equilibrium is less shifted and *(ii)* due to its less-packed structure, structural rearrangements could be more easily induced. However, it has also to be considered that the side-chain of H337 is located within the presumably binding site; hence, the mutation R337H might directly influence the interaction.

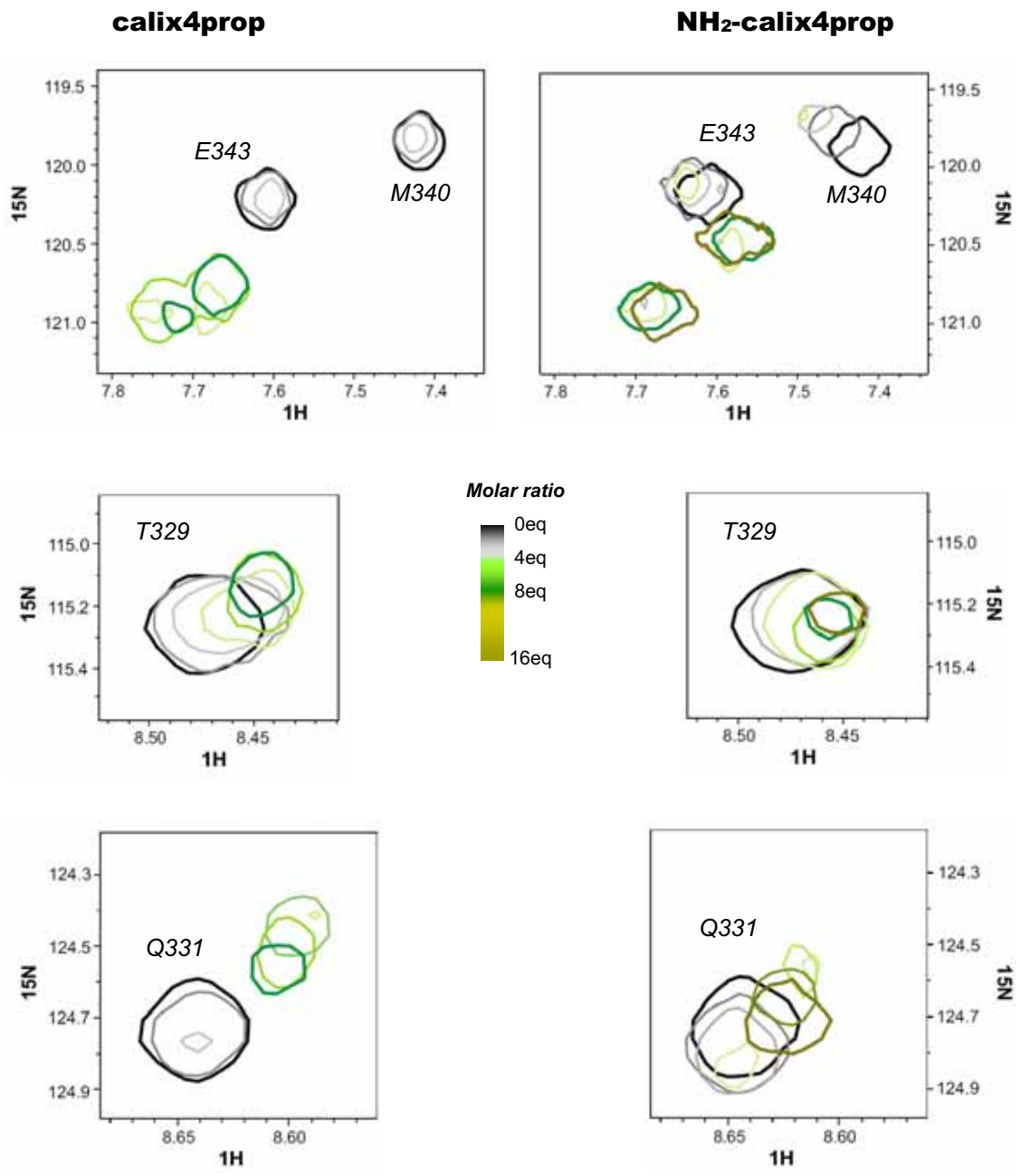

Figure 3.14. HSQC evolution of some **R337H** resonances during titration with **calix4prop** (left panels) or **NH_2-calix4prop** (right panels). In black, the free protein (125μM tetramer, in water pH 7.04 at 298K); in the grey scale, up to 4 molar equivalents of ligand; in the green scale, from 4 to 8 molar equivalents; in the khaki scale, up to 16 equivalents.

As with p53wt, mutant R337H also was titrated with NH_2-calix4prop, and the results are in agreement with the aforementioned hypotheses. The overlapped spectra for the titration are provided in the Supplementary Material, and the details for some resonances are presented in **Figure 3.14**, where they can be compared with those from the titration with the tetraguanidinium-calix4prop. As predicted, the amino-ligand displayed lower affinity, and some minor shifts of the protein resonances were detected at the lowest ligand ratios (assuming that the perturbation distances, Δδ, were similar for both ligands). The initial shifts were accompanied by a decrease in

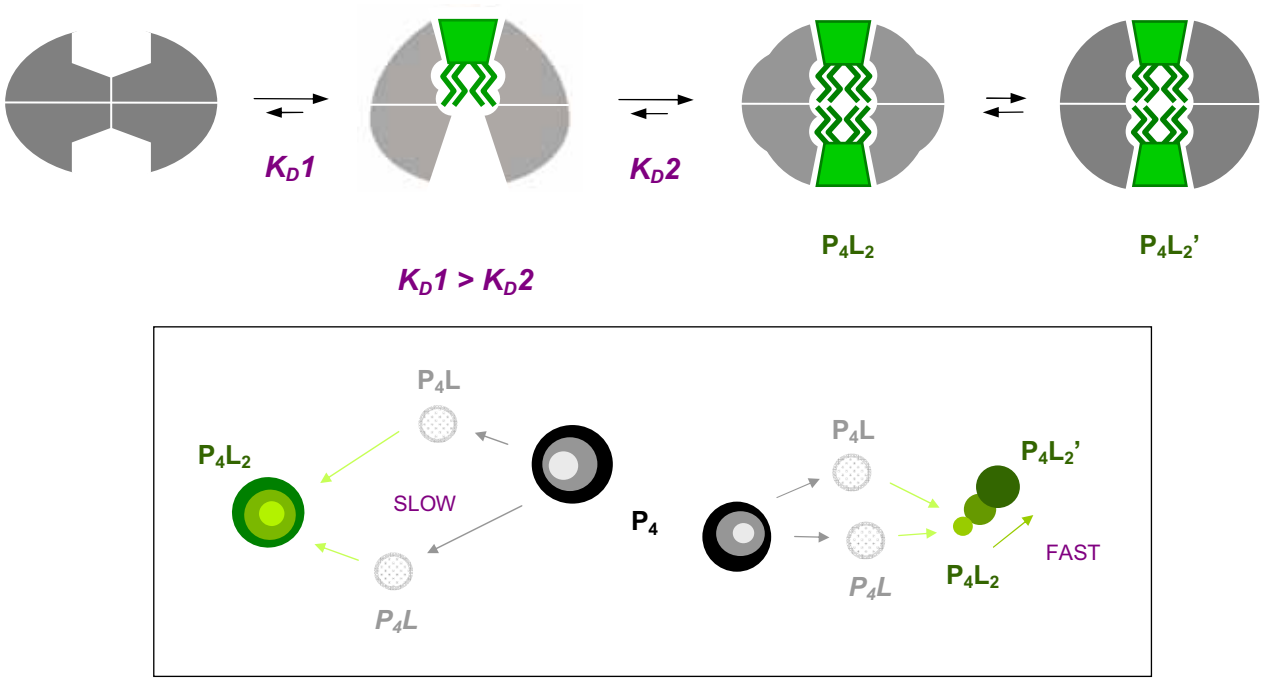

Figure 3.15. Hypothetical sequential positively-cooperative binding mechanism for two molecules of **calix4prop** to **R337H**, with structural rearrangements. The lower panel represents the evolution for two HSQC resonances: one is affected only by the binding (left) and the other undergoes some minor structural modifications after the second binding (right).

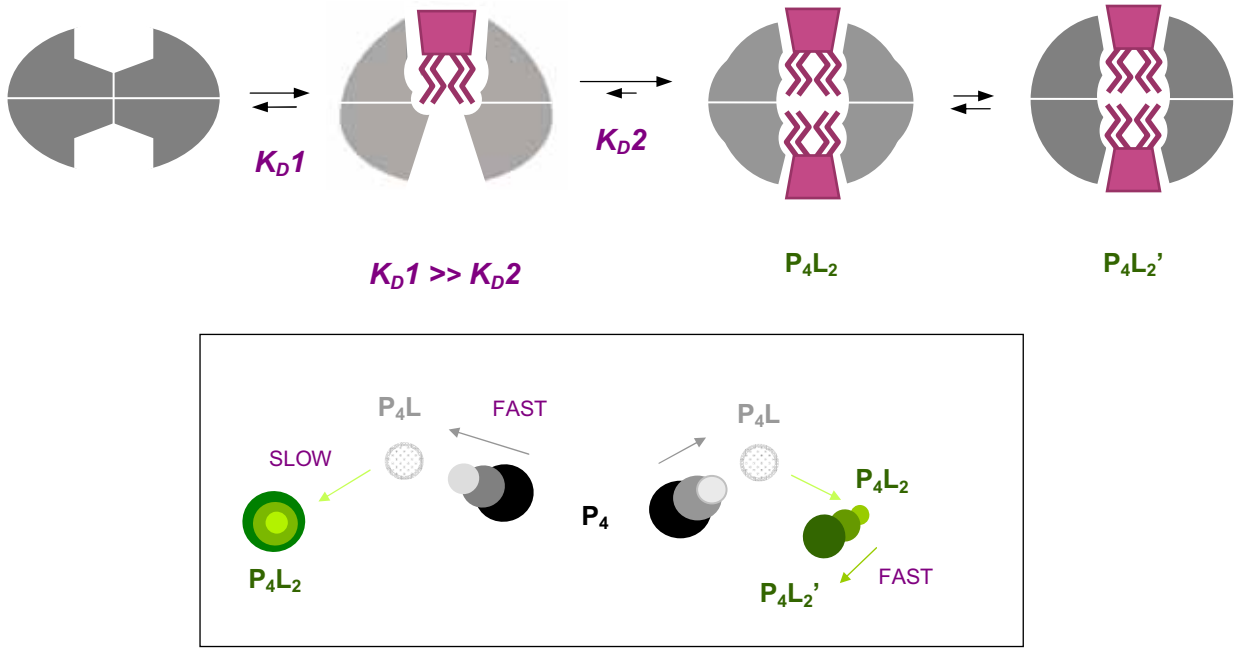

Figure 3.16. Hypothetical sequential cooperative binding mechanism for **NH_2-calix4prop** to **R337H**. The lower panel represents the evolution for two HSQC resonances: one is affected only by the binding (left) whereas the other undergoes structural modifications after the second binding (right).

intensity and former peaks were vanished at 4 equivalents of ligand. The new set of resonance then emerged, and, as was described for p53wt, not all of the new peaks appeared in the same location as in the guanidinium-calix4prop. Shifting of some of the new resonances also was detected, but it required higher ligand excesses, and perturbation was lesser.

The mechanism by which NH_2-calix4prop interacts with R337H (**Figure 3.16**) is compatible with that proposed for the tetraguanidinium-ligand, but presumably with lower affinity. The third event, the suggested structural rearrangement, proceeded to significant far lesser extent, which could also be consistent with the lower affinity displayed by the amino-groups. However, an alternative third binding event could not be ruled out from these results.

(c) Mutant G334V

The tight binding of calix4prop with p53wt and R337H detected by NMR was in agreement with the ligand-induced thermal stability detected by DSC. However, thermal stabilization was not observed for mutant G334V, which in the presence of calix4prop displayed a peculiar structural transformation at high temperatures.

Titration of ^{15}N-G334V with calix4prop at room temperature did not lead to any large change of the HSQC spectrum (full spectra provided in the Supplementary Material). In fact, as seen in the details from **Figure 3.17**, the perturbation of G334V resonances in the presence of calix4prop was similar to that described for the other proteins. The affinity might be somewhat poorer, and at the lower ligand concentrations, some resonances experienced a clear shift (assuming a $\Delta\delta$ comparable to that for the other proteins). At *ca.* 4 equivalents of ligand (relative to 125μM tetramer), peaks vanished, and then reappeared elsewhere; further addition of calix4prop only helped to increase their intensity.

The mechanism hypothesized for p53wt could also apply to G334V, but with presumably lower affinity in the first binding. The poorer affinity was initially surprising; G334V was not as packed as the wild-type tetramer and hence, rearrangements were expected to proceed more easily. However, the “wider” structure adopted by this mutant could also play a negative role in its interaction with calix4prop, as the binding site might not present the optimal dimensions to perfectly fit the calixarene. For instance, the guanidinium groups in the upper rim might not be able to interact tightly with the carboxylate moieties on the protein surface because they might be too apart.

When G334V was titrated with NH_2-calix4prop, all resonances evolved under a fast chemical exchange. However, not all the peaks shifted unidirectionally, and some exhibited slight bending in their trajectory (although this was not the case for the two resonances shown in **Figure 3.17**), which suggested a second binding event with affinity on the same order as the first ligand binding.

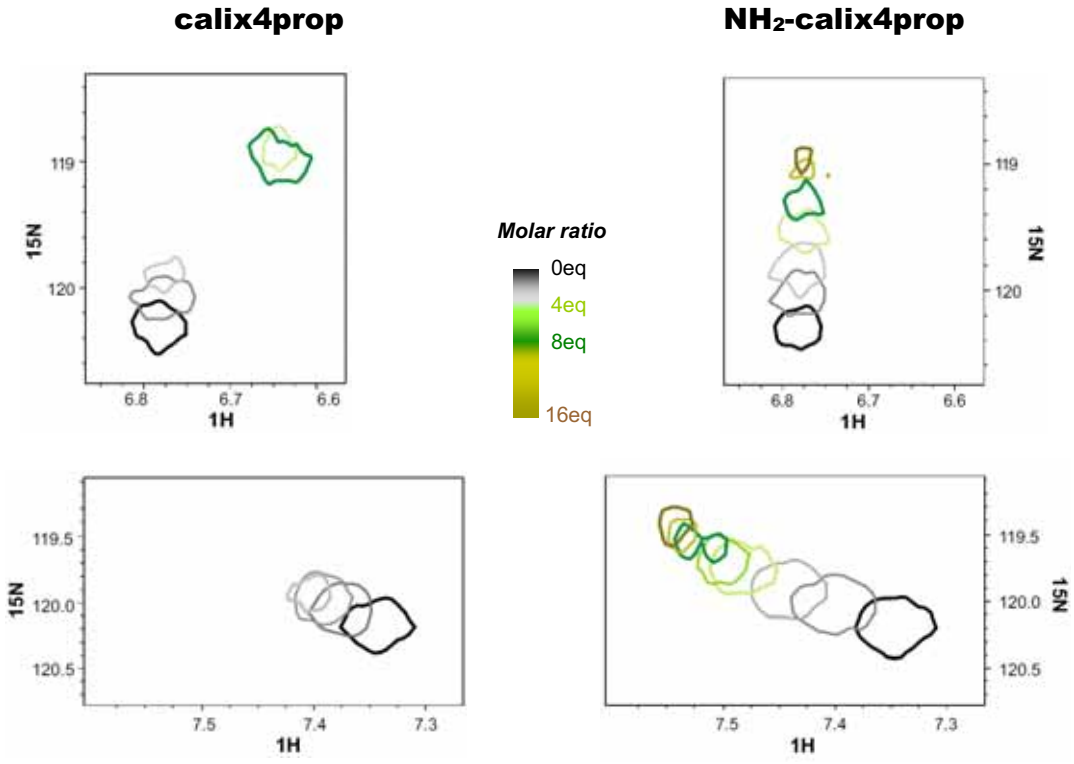

Figure 3.17. HSQC evolution of two **G334V** resonances through a titration with **calix4prop** (left panels) or **NH_2-calix4prop** (right panels). In black, the free protein (125μM tetramer, in water pH 7.04 at 298K); in the grey scale, up to 4 molar equivalents of ligand; in the green scale, from 4 to 8 molar equivalents; and in the khaki scale, up to 16 equivalents.

3.4.1.2. The role of the upper rim

Through a collaboration of de Mendoza's (*ICIQ*) and Ungaro's (*Università degli Study di Parma*) groups, we were able to obtain the tetraguanidinium calix[4]arene **4G4Pr-cone** (5,11,17,23-tetraguanidinium-25,26-27,28-propoxycalix[4]arene).[33] The lower rim of this molecule was also functionalized with four propyl groups, but it differed from our calix4prop because the guanidinium groups in the upper rim were linked directly to the aromatic ring, so it lacked the linking methylene and the basicity of its guanidinium groups was somewhat lower (the pK_a for phenylguanidine is 10.9, whereas that of benzylguanidine is ~13).

The effects of 4G4Pr-cone on proteins structure were also evaluated by NMR. Interestingly, the changes promoted by 4G4Pr-cone were identical to those described for the amino-ligand NH_2-calix4prop, as can be appreciated in the details of the HSQC spectra shown in **Figure 3.18** (compare with **Figure 3.8** and **Figure 3.9**) and in **Figure 3.19** (compare with **Figure 3.14**). The newly emerged set of resonances presented only some minor differences with the one corresponding to NH_2-calix4prop, and the ligand concentrations required to promote the changes in the spectra (*i.e.* shifts and peak disappearance) were almost the same.

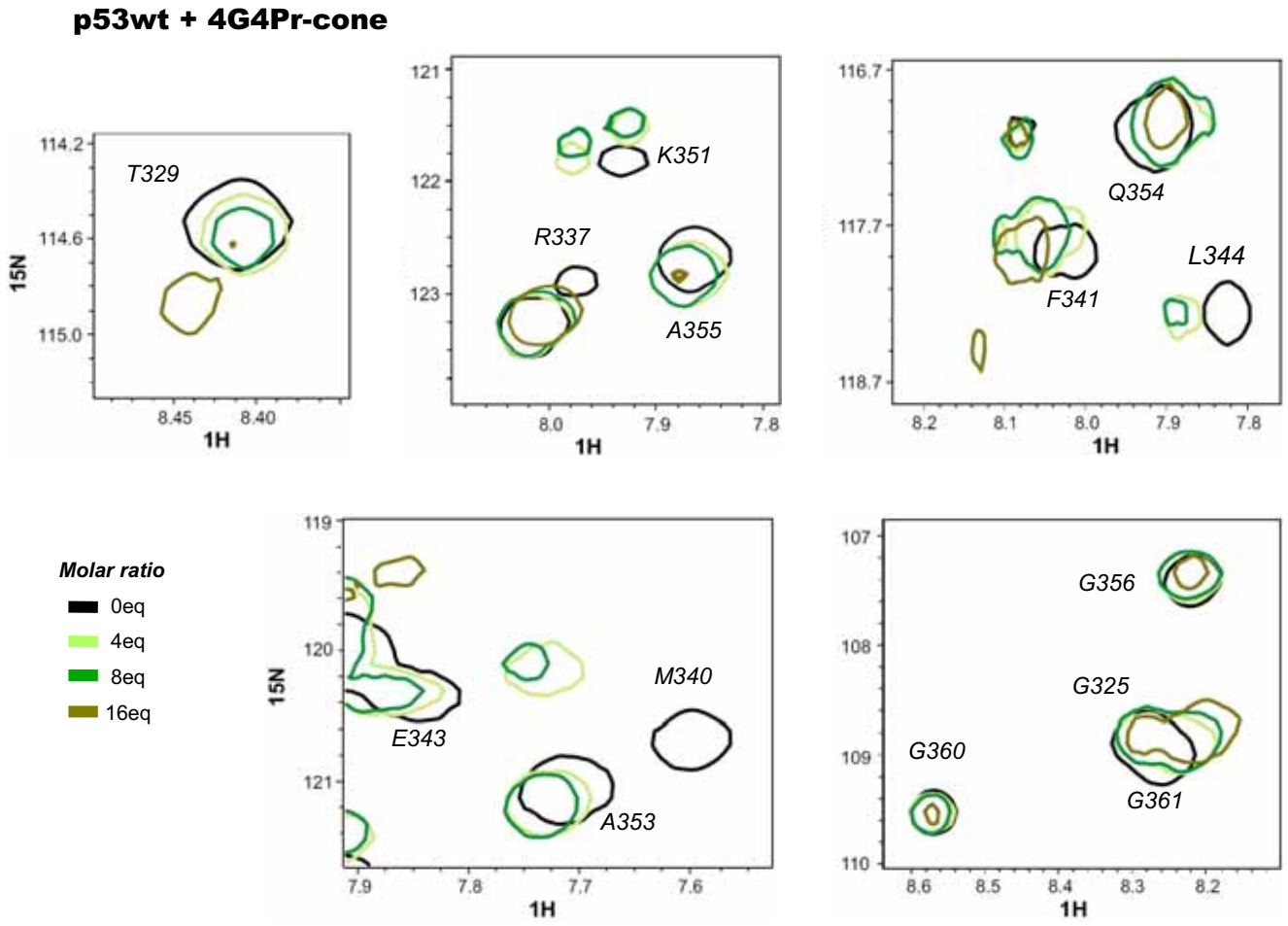

Figure 3.18. HSQC evolution of some **p53wt** resonances during titration with **4G4Pr-cone.**

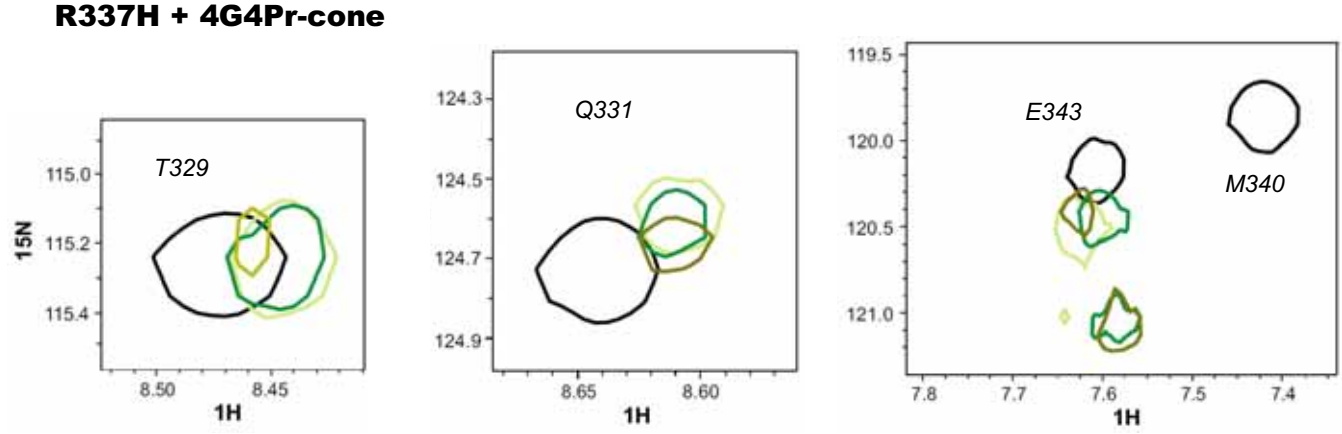

Figure 3.19. HSQC evolution of two **R337H** resonances during titration with **4G4Pr-cone**.

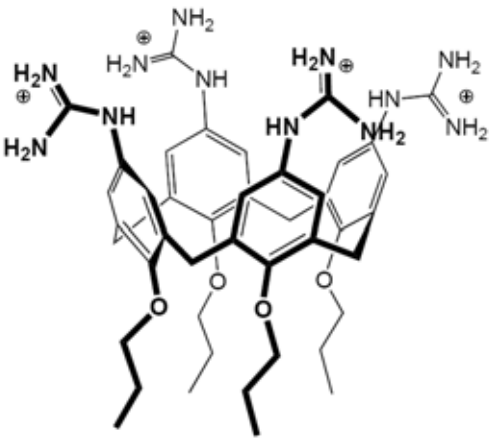

4G4Pr-cone

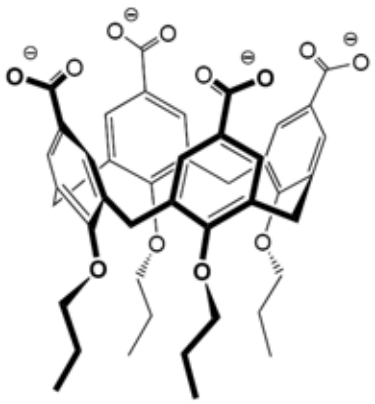

COOH-calix4prop

These results helped in understanding the crucial role of the upper rim functionalization. In comparing the three tested calixarenes (calix4prop, NH_2-calix4prop and 4G4Pr-cone), it seemed that the length of the "branch" containing the positive charge and the basicity of the positive charge itself were essential for the interaction. Positive charges attached to a short chain probably could not "reach" the carboxylate moieties on the protein surface (**Figure 3.20** and **Figure 3.21**). In addition, for less basic moieties, all four interactions probably could not be established at once. Hence, efficient and total ionic chelation was critical for tightly anchoring the ligand into the protein and, consequently, easily promoting structural rearrangements. However, said chelation was not the only driving force: hydrophobic interactions were, evidently, of utmost importance.

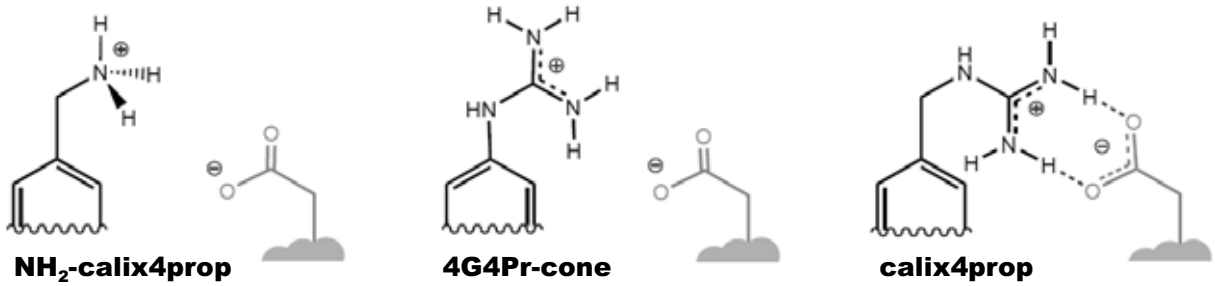

NH_2-calix4prop **4G4Pr-cone** **calix4prop**

Figure 3.20. Comparative representation of the interaction between the upper-rim and a carboxylate from the protein (hypothetical distances considering that only calix4prop could perfectly chelate the protein). Basic moieties are represented protonated, although they possess different basicity. For approximate pK_a values: benzylamine conjugated acid, pK_a: 9.3; phenylguanidina, pK_a: 10.9; benzylguanidina, pK_a: ~13. The proximity of the four groups in the calix[4]arene may lead to lower pK_as.[34,35]

In fact, the role of the distance between the positive charges in the upper rim of the calix[4]arene and the carboxylates on the protein surface has been already described from the point of view of the protein. For mutant G334V, the interaction with calix4prop was not as tight as expected for a less packed protein and that could be ascribed to the "wider" conformation adopted by G334V,

which would –presumably– place the carboxylate moieties too apart for perfect interaction with the positive charges in the calixarene upper rim (**Figure 3.21**).

COOH-calix4prop, a calix[4]arene in which the propyl groups in the lower rim were maintained, but whose upper rim was functionalized with four carboxylic acids directly bound to the aromatic ring (HSQC spectra are provided in the Supplementary Material), was employed as negative control. Interaction with the carboxylate groups from the protein was thus avoided, but considering the large number of positive residues on the protein surface, the carboxylates from the calixarene might have established interaction with them. However, that was not the case. In fact, COOH-calix4prop behaved as a detergent, generating foam when the sample was mixed and denaturing and precipitating the protein.

In conclusion, positive charges were determined a requisite for maintaining the molecular capability of the calix[4]arene with four propyl groups in the lower rim.

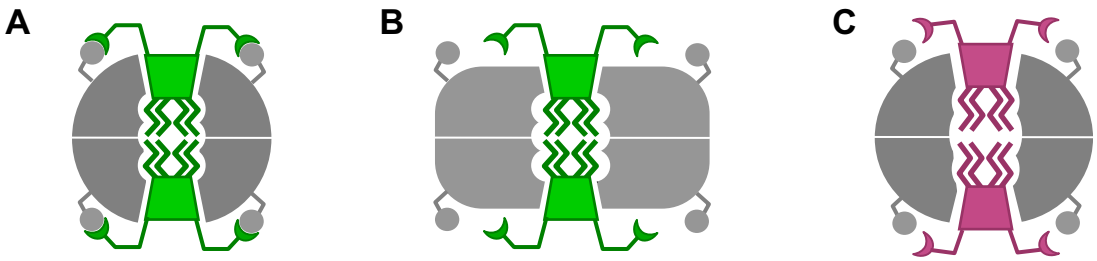

Figure 3.21. (A) Schematic representation of the perfect chelation between the guanidinium groups of calix4prop and the carboxylates moieties on protein surface (grey balls). **(B)** The less compact structure of G334V, places –presumably– the carboxylates too apart from the ligand binding site, making efficient ionic chelation impossible. **(C)** Substitution of the guanidinomethyl by a shorter group (*i.e.* guanidinium or aminomethyl) would not allow establishment of a strong interaction, either.

3.4.1.3. ^{1}H up-field perturbation

The significant changes in the HSQC spectra suggested important structural rearrangements of the protein upon interaction with calix4prop. In order to assess this hypothesis, the up-field region of the ^{1}H-spectrum of the protein was analyzed. Resonances in this region correspond to protons from the protein side-chains which are close to an aromatic ring current and therefore very sensitive to conformational changes.[36-38] The results for the titration of protein with calix4prop and with NH_2-calix4prop are summarized in **Figure 3.22**.

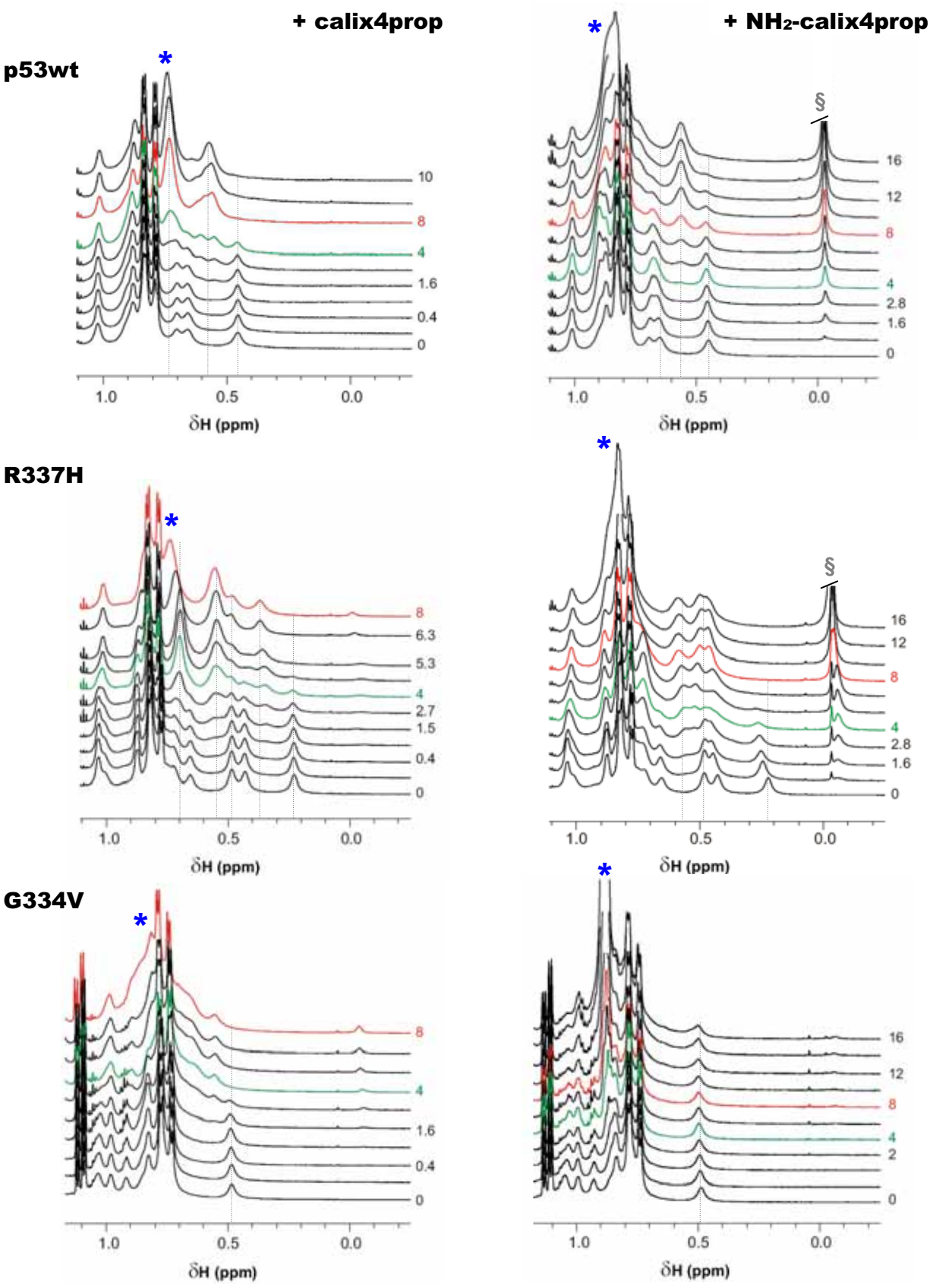

Figure 3.22. Up-field ^{1}H-resonances progress during the titration with calix4prop (left panels) and NH_2-calix4prop (right panels) for p53wt (top), R337H (middle) and G334V (bottom). Ligand molar ratios (relative to the tetramer) are indicated at the right of the spectra. For clarity, spectra at 4eq of ligand are colored green and those at 8eq in red. Possible emerging methyl-ligand resonances are indicated by a blue asterisk. The § peak corresponds to a minute impurity from the ligand.

As expected for a conformational change, calix4prop and NH_2-calix4prop affected all up-field resonance. The progress of the resonances perfectly correlated with the chemical exchange kinetics described for the HSQC. The simplicity of a one-dimensional spectrum better displayed when the new resonances emerged; the ligand ratios agreed with the qualitatively estimated affinities: R337H (assuming a slow dissociation, then, $K_D \lesssim$1-10μM) > p53wt ~ G334V. Resonances at the end of the titration were broader, as would correspond to the multiple, slow binding equilibriums coupled to structural changes.

Upon interaction of the protein with the ligand, conformational changes could lead to the disappearance of previous up-field resonances (*i.e.* as the aromatic ring and its closest protons separated) as well as the apparition of new ones (*i.e.* as the protein aromatic rings approached other protons). Moreover, considering the aromatic nature of the calixarene platform and the tightness of the ligand binding, new resonances could even result from close positioning and proper orientation of protein protons to the calixarene ring currents. Indeed, it is worth noting that for p53wt and R337H, a broad, intense, new peak emerged at *ca.* 0.55ppm. Perhaps, this new resonance was the result of the ligand ring-currents, and if it was common for all the proteins, it might suggest a similar ligand-protein interaction.

Nevertheless, those are just hypotheses. Analysis of the up-field region led to deduction of the major structural rearrangements, but little else.

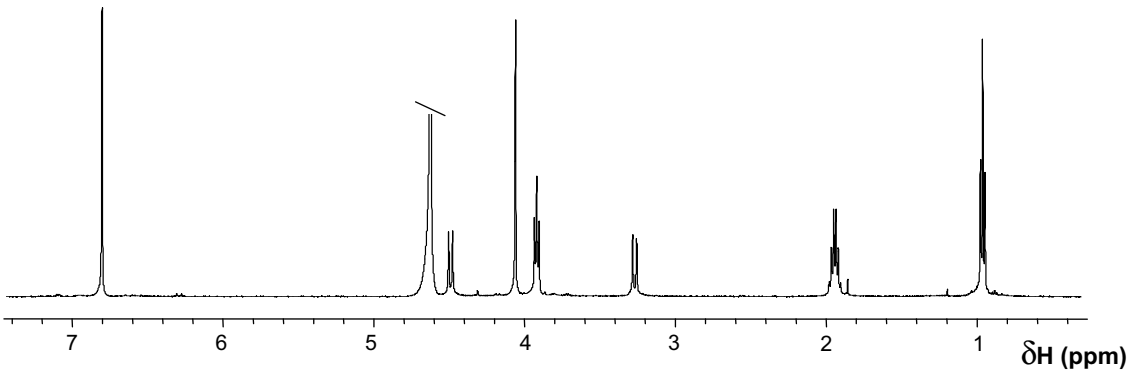

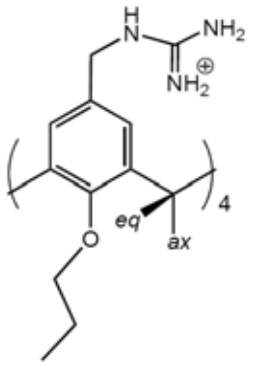

	δ_H (ppm)	*J* (Hz)	H
aromatics	6.797		8
Ar-**CH2**-Ar **axial**	4.473	21 (d)	4
Ar-**CH2**-NH-	4.037		8
Ar-O-**CH2**	3.898	13 (tri)	8
Ar-**CH2**-Ar **equatorial**	3.249	21(d)	4
CH2-CH3	1.925	13 (m)	8
-CH3	0.927	13 (tri)	12

Figure 3.23. ^{1}H spectra of calix4prop (600MHz, D_2O “99.99%”, 298K).

3.4.2. NMR on the ligand

From the structural information provided by the HSQC experiment on the protein, little could be determined about how calix4prop interacted with p53 tetramerization domain. Determining the ligand binding mode was invaluable for understanding the molecular recognition event; hence, NMR experiments on the ligand were performed.

3.4.2.1. ^{1}H spectrum

One of the most important features of the structure of calix4prop is it symmetry, which is of higher order than that of the p53 tetramerization domain. Therefore, upon interaction with the protein, calix4prop should become asymmetric, as illustrated in **Figure 3.24**.

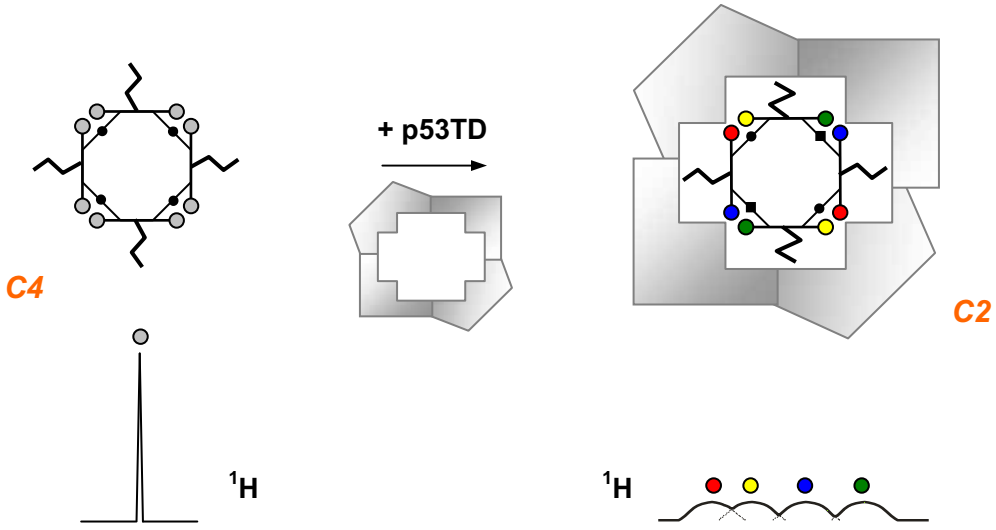

Figure 3.24. Schematic representation of free calix4prop (symmetry *C4*) and bound to the hypothetical protein binding site (symmetry *C2*). Despite the fact that the ligand interaction causes structural rearrangements, protein symmetry is most likely preserved. Equivalent aromatic protons of calix4prop are represented as balls of the same color. The hypothetical split and broadening of the ^{1}H resonance for these nuclei are illustrated at the bottom.

The slow chemical exchange that the protein-ligand system underwent led to the expectation that the changes in the spectra of calix4prop in the presence of p53 would be highly intricate; firstly, because resonances for the bound-form would be extremely broad, and secondly, because ligand resonances would multiply split as a result of the symmetry loss.

Furthermore, many of the calixarene resonances were close to the water band, and the use of sequences with pre-saturation pulses to suppress water would further complicate the analysis of

ligand resonances (see section 2.3.2.1). Hence, even if calix4prop were in large excess, ligand resonances might not be easily detected or interpreted.

In fact, close inspection of the ^{1}H spectra of the proteins when titrated with calix4prop hardly revealed anything about the ligand resonances. The least ambiguous changes were detected in the up-field region, in which there were only a few well-defined protein resonances that did not "bury" the broad, emergent methyl peak from the calixarene (as shown in **Figure 3.22**). Presumably, that peak should correspond to the free ligand, which was in excess at the largest ratios. Given that the protein-ligand interaction was reversible, ligand resonances could still bear some information (*i.e.* on the chemical shift and the line-broadening) about the bound state. That would explain why the resonance emerged at higher fields (~0.7ppm) than expected for the free ligand (~0.95ppm). In contrast, for the amino-ligand NH_2-calix4prop the methyl peak emerged nearer to the free-ligand location (~0.85ppm), which would agree with the hypothesis of looser binding.

The titration of calix4prop with protein did not help in understanding what had occurred with the ligand resonances: once the free ligand resonances had disappeared, the new ligand-bound peaks could not be identified.

3.4.2.2. Transferred nOe

The inappropriate location of the ligand resonances, widely spread along the whole ^{1}H-range (**Figure 3.23**), made STD experiments on calix4prop impossible since, whatever the frequency selected to irradiate the protein, the ligand was also saturated. The recently reported ^{15}N-group selective STD experiment,[39] whereby the amide protons of a ^{15}N-labelled host are selectively saturated, was not suitable either because calix4prop has exchangeable protons that might be non-specifically affected. However, even if selective saturation of the protein had been possible, STD might have failed because of the rather slow dissociation rate of the calix4prop-protein complexes.

Despite the fact that transferred nOe experiments are more convenient for weakly binding ligands (*i.e.* a singlet set of resonances, $K_D > 10^{-7}$M and $k_{off} > 1/T1$),[40-42] some preliminary NOESY and ROESY spectra of calix4prop with and without protein were performed. Although these did not comprise a complete study, the initial results are noteworthy.

The first most relevant feature –and a clear indicator of protein interaction– was the change in sign and intensity of the nOe cross-peaks for calix4prop (**Figure 3.25**, upper panels): small and positive for the free ligand (as corresponds to a small-medium size molecule), and large and negative in the presence of protein (as corresponds to a large protein-ligand complex).[43] No clear new cross-peaks were detected in the NOESY spectrum (for a sample containing 500μM of ligand and 12.5μM p53wt tetramer).

The intensity of the ROESY spectrum also increased when the protein was added, although no change of sign was observed (**Figure 3.25**, lower panels); that suggested that all cross-peaks corresponded to direct nOes and not to spin-diffusion. Interestingly, a new cross-peak was detected in the ROESY spectrum of the protein-bound ligand, between the axial proton in the Ar-CH_2-Ar and the second methylene of the lower-rim propyl chains (**Figure 3.26**). This led to the thought that calix4prop might interact with the protein in a preferred conformation in which free propyl chains would somehow rearrange upon fitting of the ligand into the protein pocket.

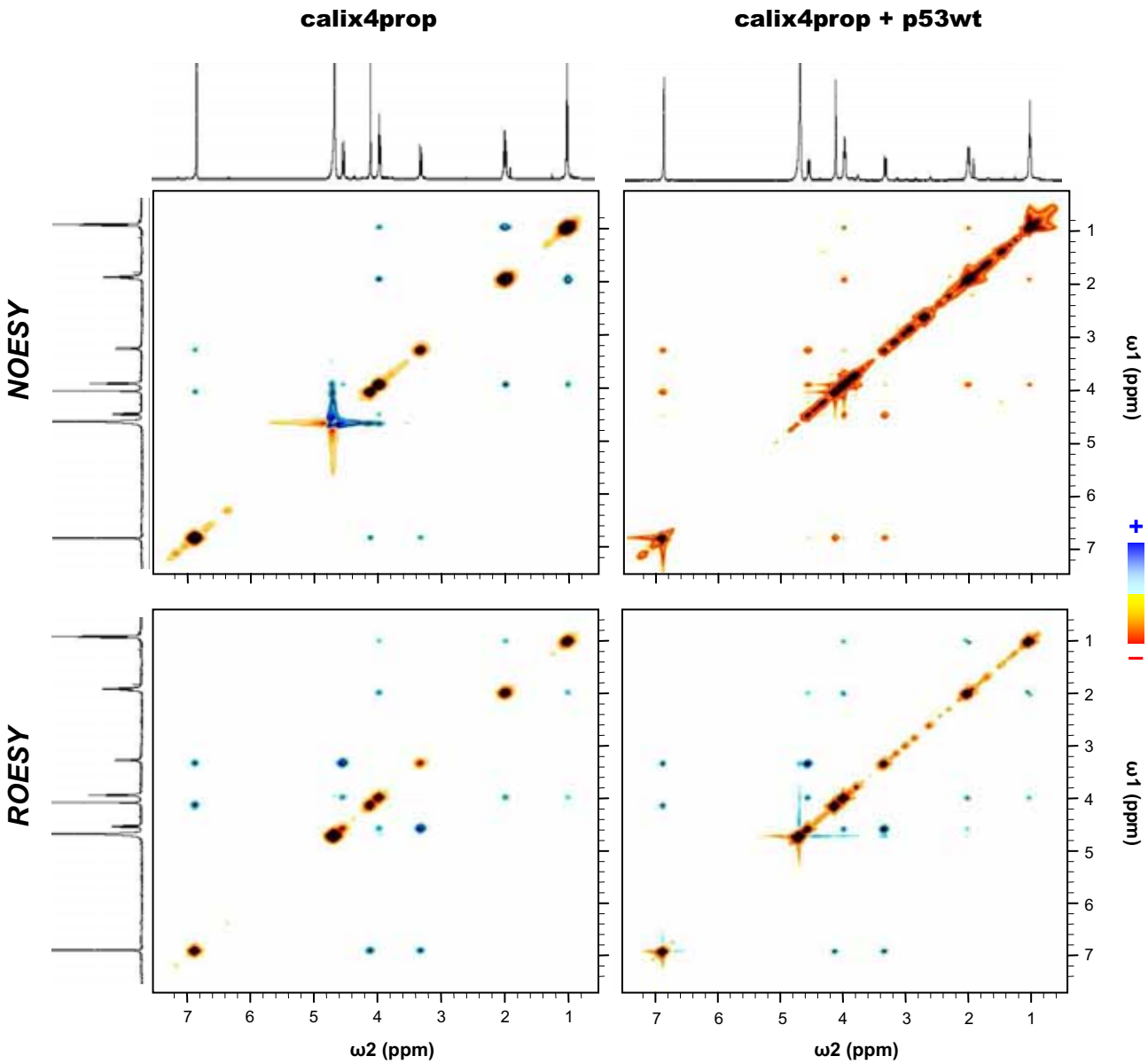

Figure 3.25. NOESY and ROESY spectra of 500μM calix4prop, free (left) and in the presence of 12.5μM p53wt (right). The ^{1}H spectra represented at the top correspond to the respective samples while those at the left correspond only to the free ligand. Despite the fact that samples were prepared in "99.99%" D_2O, the NOESY spectra were recorded with water suppression; therefore some cross peaks surrounding the water band were not clearly detected (308K, 500MHz).

The low quality of the data and the limited number of experiments performed in this preliminary study did not allow further mathematical treatment of the NOESY/ROESY; hence, it was not possible to estimate the bound-ligand conformation sought. In addition, nOe cross-peaks were cross-contaminated with spin-diffusion and TOCSY effects (especially those from the propyl chain), which would further prevent the interpretation of the current experimental results[d].

Despite the limited information, the change of nOe sign strongly supported that calix4prop interacted with p53TD. Furthermore, the detection of a new cross-peak in the ROESY spectrum suggested that the binding favored a particular conformation of the ligand.

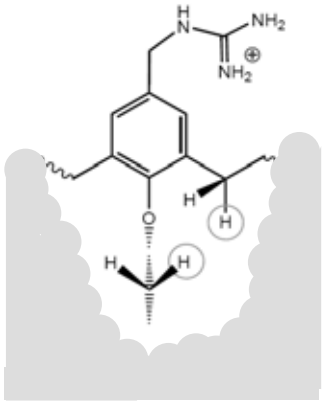

Figure 3.26. New direct tr-nOe

Transferred nOe experiments were also recorded for samples with lower ligand excesses (adding protein to get ratios of 20 and 10 equivalents of ligand) in order to determine if it was possible to detect cross-peaks between both molecules. The NOESY spectrum at higher protein concentrations (provided in the Supplementary Material) changed substantially and became difficult to interpret. Since the protein and the ligand underwent a slow chemical exchange, at lower molar ratios the free and bound ligand resonances co-existed, and the number of cross-peaks increased. Additionally, from the limited experimental data, it was difficult to determine if cross-peaks pertained to intra- or inter-nOes.

These tr-nOe preliminary results neither confirmed nor ruled out the binding hypotheses suggested in previous sections. Further experiments, under optimal conditions, are therefore required. Better results would probably be obtained from evaluation of the amino-ligand NH_2-calix4prop; although its second binding is also a slow exchange equilibrium, the first one might be fast enough as to improve tr-nOe detection.

[d] There exist pulse sequences which remove the TOCSY contamination from ROESY cross-peaks, however these were just preliminary experiments and they were not used. Spin-diffusion effects can be controlled by evaluation of the tr-nOe build up curve, which further provide information on the ligand binding mode, but in those preliminary experiments it was not performed a thorough study on the mixing time.

3.5. Isothermal Titration Calorimetry

The thermodynamic characterization of the interaction with calix4prop was also approached by ITC. Unfortunately, the experimental limitations made the ITC results not accurate for analysis.

The main source of experimental uncertainty in the calorimetric data arose from the unsuitability of water for ITC. As discussed in section 2.4, one of the main drawbacks of working in plain water is the impossibility to match buffers from the cell and the syringe, thus maximizing the dilution heat.[44] In addition, this large dilution heat could not be properly corrected with a blank dilution experiment over water. The synthetic origin of the calixarene further worsened the problems. These inconveniences are illustrated in **Figure 3.27**. The large endothermic dilution heats for the ligand might suggest the existence of non-covalent intermolecular aggregates[45] in the stock solution, which could be due to the amphipathic nature of calix4prop.

A titration over the negative control L344P helped in assessing the effects of diluting the calixarene into a crowed self-buffered protein solution (**Figure 3.27**). As corresponds to a partially non-polar molecule, the dilution in a higher ionic strength solution was more exothermic (but still endothermic). The irregular profile could be the result of unspecific interactions as well as inaccuracy in the data processing.

The ITC results for p53wt, R337H and G334V in these preliminary experiments are shown in **Figure 3.28**. Despite the uncertainty associated to the experimental data, the heat recorded for the interaction with calix4prop was large enough as to distinguish two energetic processes, being the second event more exothermic than the first one.[46] In fact, it appeared as if the process taking place at the lower ligand ratios was endothermic. Around 4-6 equivalents of ligand (relative to tetramer) the binding energy reached a minimum and the second energetic event became dominant. Said molar ratios were similar to the already described for the NMR changes (if they were slightly larger it could be because the lower concentrations now used). The differences detected between the three proteins also agreed with the affinities approximated by NMR: R337H presented higher affinity than p53wt and G334V. Saturation was apparently reached at the end of the titration, although the dilution heats were not null; that was probably due to the differences in ionic strength between the water blank dilution and the protein sample.

The lack of reliability of these experimental results made impossible to obtain trustworthy information about the thermodynamics of calix4prop interaction, although the two detected process would correlate well with other results.

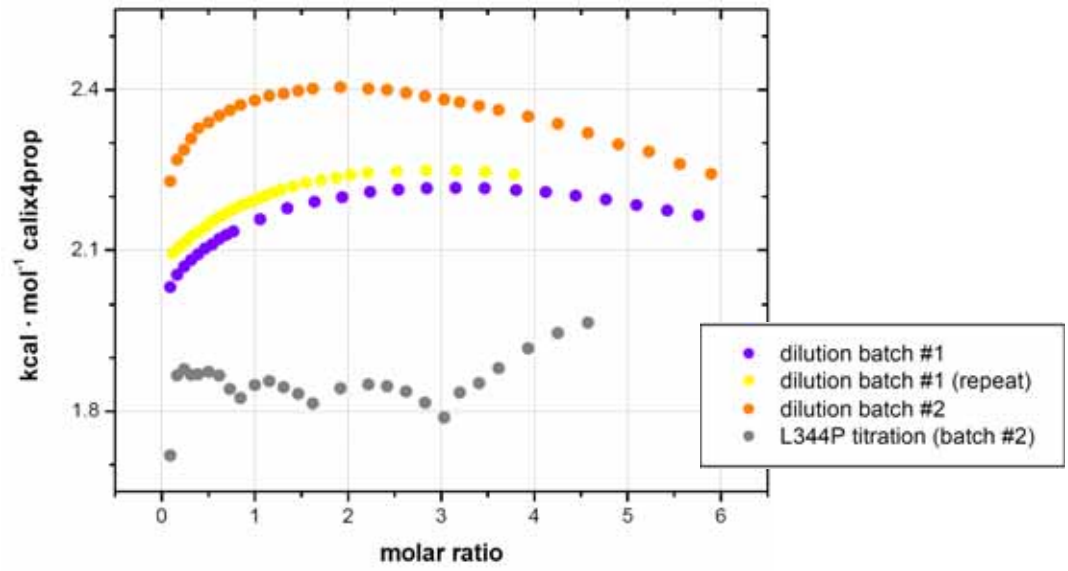

Figure 3.27. Inconveniences of working in water. Dilution titration of two different synthetic batches of calix4prop into water led to different values of endothermic heat (● and ● vs. ●). Moreover, dilution heats were not reproducible for a given batch (● vs. ●). Titration into 200μM L344P (●), *i.e.* a crowed self-buffered protein solution, resulted in a different, irregular profile. Molar ratios calculated based on 200μM of protein. In water at pH 7.0 and 25ºC.

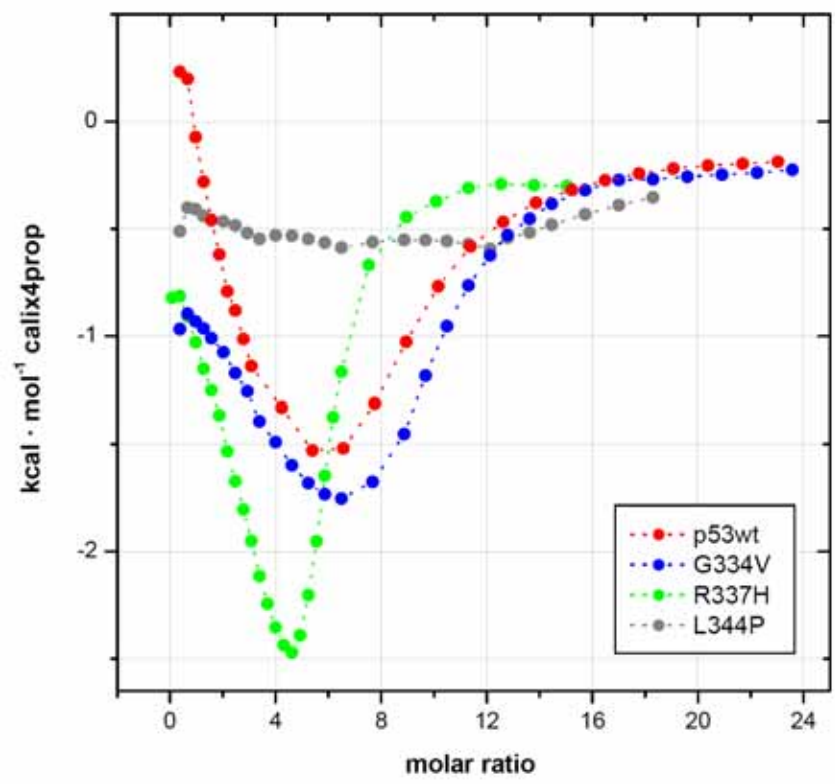

Figure 3.28. ITC results of calix4prop and p53wt (●), R337H (●), G344V (●) and L344P (●), once the corresponding water blank dilution was subtracted. Molar ratios relative to 50μM of tetramer (although the tetramer for L344P does not exists, it allows comparison with the other proteins). Experimental points have been connected (dashed line) to better follow the progress. In water at pH 7.0 and 25ºC.

3.6. Towards the detection of the tetrameric complex

3.6.1. Chemical cross-linking

The results presented thus far agree with a model in which two molecules of calix4prop strongly interacted with p53TD, and the ligand binding further promoted a structural rearrangement on the protein. Before mass spectrometry provided the most striking evidence that calix4prop was interacting with a tetrameric assembly, chemical cross-linking experiments were done and their interesting results are worth to be discussed.

When glutaraldehyde was used to covalently cross-link proteins in the presence of calix4prop (**Figure 3.29**), the band corresponding to the tetramer was clearly intensified. Bands for the monomer and the trimer nearly disappeared, whereas the dimer band remained almost the same. In agreement with the affinity order, changes in R337H proceeded more readily than for p53wt or G334V.

The increase of cross-linked tetramers supported the proposed interaction model, with the tetramer ensemble "stabilized" by calix4prop. Moreover, it could even suggest that the ligand-induced structural rearrangements on the protein were somehow affecting the location of the lysine side-chains; hence, they might become better oriented to be easily cross-linked. The rearrangements could only affect K351 (within the native packed tetramer) but changes in the unfolded terminal tails (affecting K319/K320/K321, in the N-terminal tail, or K357, in the C-terminus) could not be ruled out.

For G334V, glutaraldehyde cross-linking (at 37ºC) in the presence of calix4prop showed a shift towards the tetrameric oligomer (**Figure 3.30**), just as the other protein did. Performing the experiment at higher temperatures –adding before or after the cross-linker– did not lead to any different pattern that could suggest aggregation. However, that was not surprising, since all the parameters critical for the "β-re-folding" process (*e.g.* protein concentration, presence of glutaraldehyde, glycerol, and uncontrolled pH) changed in the cross-linked samples.

For mutant L344P, a monomeric unstructured chain, some high order oligomers were cross-linked when calix4prop was added to the sample (**Figure 3.30**). Those species were most likely due to an non-specific aggregation. Indeed, L344P precipitated in the presence of calix4prop (as was visually detected in the NMR samples).

The proteins were also cross-linked by EDC+NHS (**Figure 3.29**) and, curiously, opposite results to those of the glutaraldehyde were observed. Increasing amounts of calix4prop made the oligomers disappear, and finally, only the monomer was detected. These changes could be rationalized by two scenarios. In the first, the strong chelation of the guanidinium groups from the ligand to the carboxylates moieties of the protein might act as a shield that prevents the reaction of the carboxylates with EDC+NHS, and therefore, the cross-linking; whereas in the second, the

structural rearrangements on the protein could negatively affect the location of carboxylates and amines, thus preventing their reaction.

To better understand the different profiles exhibited by the different cross-linkers, the amine-ligand NH_2-calix4prop was also evaluated (**Figure 3.31**).

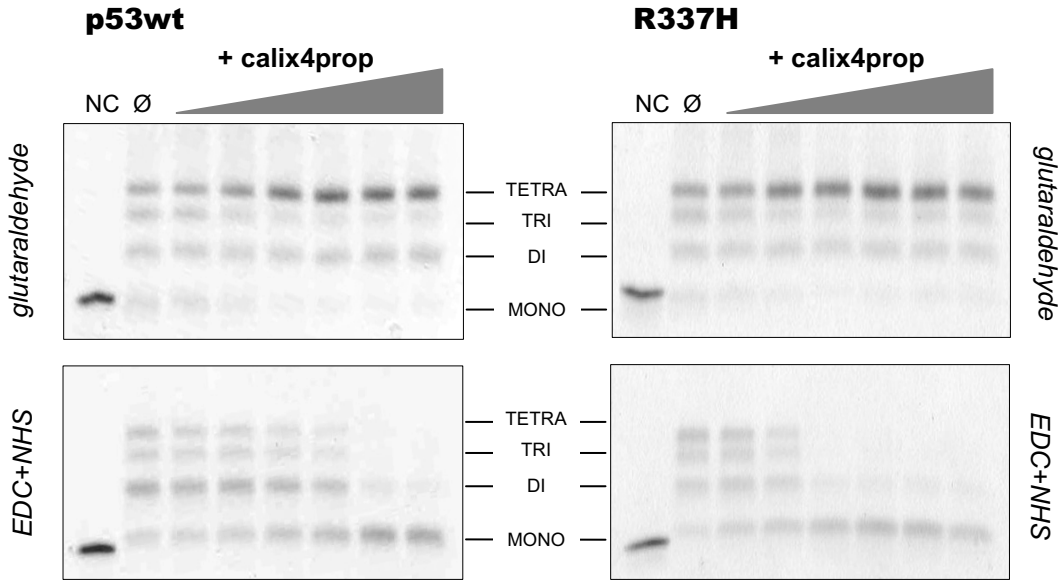

Figure 3.29. SDS-PAGE analysis of cross-linked samples of 25μM (tetramer) p53wt (left) and R337H (right) in the presence of calix4prop (ligand-to-tetramer molar ratios: 0.8, 2, 4, 6, 8, 16) using 0.1% glutaraldehyde (top) or 20mM EDC + 5mM NHS (bottom), for 25 minutes at 37ºC. NC: non-cross-liked protein. Ø: cross-linked protein without ligand.

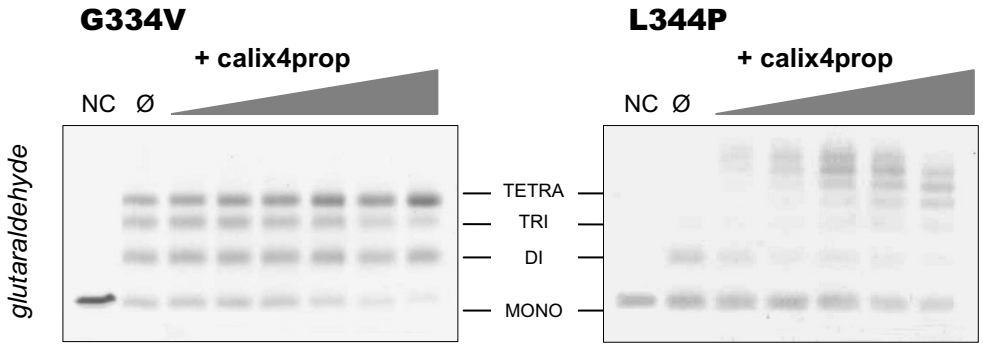

Figure 3.30. SDS-PAGE analysis of cross-linked samples of 25μM (tetramer) G334V (left) and 100μM L344P (right) in the presence of calix4prop (ligand-to-tetramer molar ratios: 0.8, 2, 4, 6, 8, 16) using 0.1% glutaraldehyde, for 25 minutes at 37ºC. NC: non-cross-liked protein. Ø: cross-linked protein without ligand.

Employing EDC+NHS, the same shift towards the monomer was detected. This strongly supported the hypothesis of the structural rearrangement. However, no intermolecular cross-linking between ligand and protein was observed. This could suggest that the amino groups from the ligand and the carboxylates from the protein might not be close enough to react (**Figure 3.21**). As expected for a lower affinity interaction, larger ligand ratios were required to detect changes.

When glutaraldehyde was used, the bands-pattern became complex, and high molecular weight species appeared (**Figure 3.31**). The most likely explanation for this was the non-specific reaction of the amino groups of the ligand, which was at high concentrations.

In conclusion, despite the limitations of the experimental procedure, and the caution which should be taken in interpreting the results, chemical cross-linking enabled rough confirmation that the protein indeed interacted with calix4prop as a tetramer.

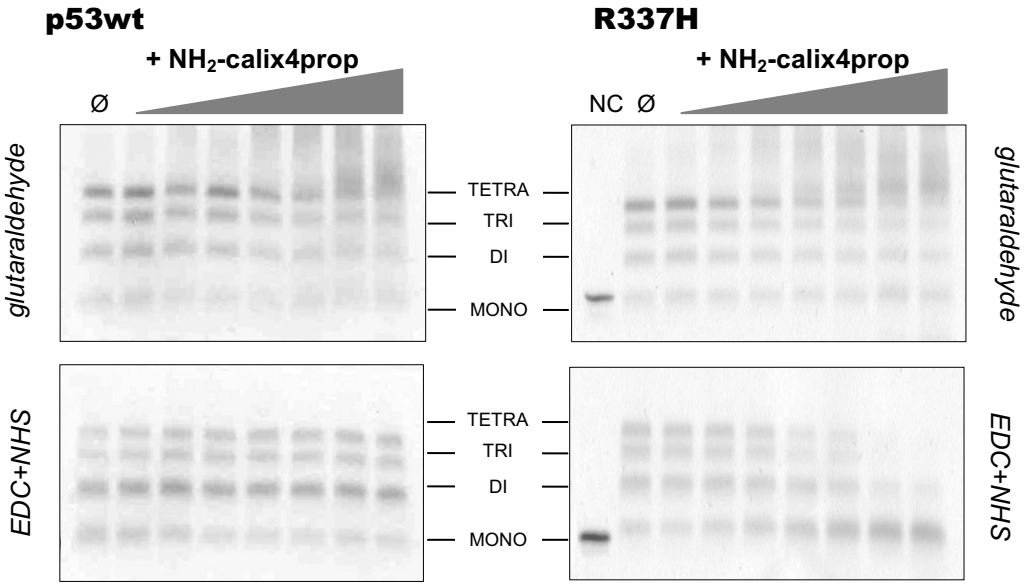

Figure 3.31. SDS-PAGE analysis of cross-linked samples of 25μM (tetramer) p53wt (left) and R337H (right) in the presence of NH_2-calix4prop (ligand-to-tetramer molar ratios: 0.8, 2, 4, 6, 8, 16, 24) using 0.1% glutaraldehyde (top) or 20mM EDC + 5mM NHS (bottom), for 25 minutes at 37ºC. NC: non-cross-liked protein. Ø: cross-linked protein without ligand.

3.6.2. Mass spectrometry

The results from the several biophysical techniques were compatible with the hypothesis that two molecules of ligand bind to the tetrameric protein. The ultimate experimental evidence which further supported said hypothesis was the detection of the complex by ESI-MS (**Figure 3.32** and **Figure 3.33**). These experiments were very preliminary –but successful– trials; the conditions for the ionization and detection were not completely optimized; hence, the results should be treated cautiously.

For the wild-type p53TD and for mutant G334V, the amount of non-covalent protein-ligand complex detected was little, but the broad peaks for the protein with one and with two bound ligands could be appreciated (**Figure 3.32**). From the experiments done in solution-phase, the affinity was estimated to be high; then, if the complex was not predominant in the gas phase, that would highlight the importance of hydrophobic interactions for the binding,[47] especially for the second binding site.

Interestingly, the opposite was observed for R377H (**Figure 3.33**).The free protein was the minor species and the tetrameric complex with one or two molecules of bound ligand the major ones. Besides the higher affinity, those differences with the other proteins could be also explanied considering that for R337H the electrostatic component was larger. That is to say, the interaction between the guanidinium groups of the ligand and the carboxylates from the protein was better established; then, in the gas-phase, the ionic chelation was further strengthened and the complex was better detected. This does not imply that the hydrophobic component was not important for the interaction R337H-calix4prop; it simply indicates that, in the hydrophobic-electrostatic balance (in the gas-phase) the electrostatic component for R337H would have larger weight than for the other proteins.

Experiments with the negative control L344P let to the detection of some dimeric species bound to one molecule of ligand, likely resulting from unspecific electrostatic interactions, which were also detected in other experiments (see Supplementary Material for spectra).

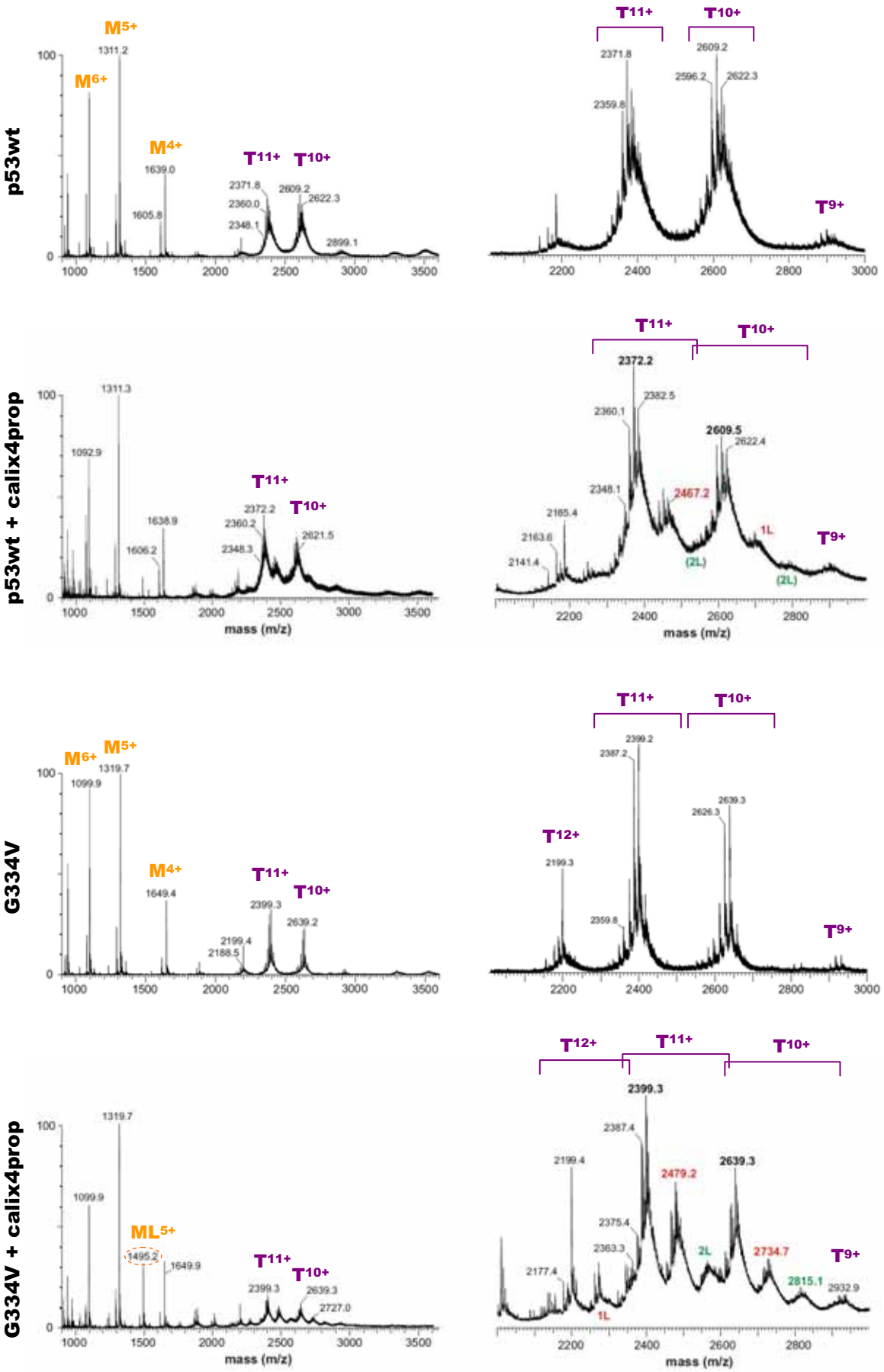

Figure 3.32. ESI-MS spectra of 50μM (monomer) p53wt and G334V in the presence of 130μM calix4prop.

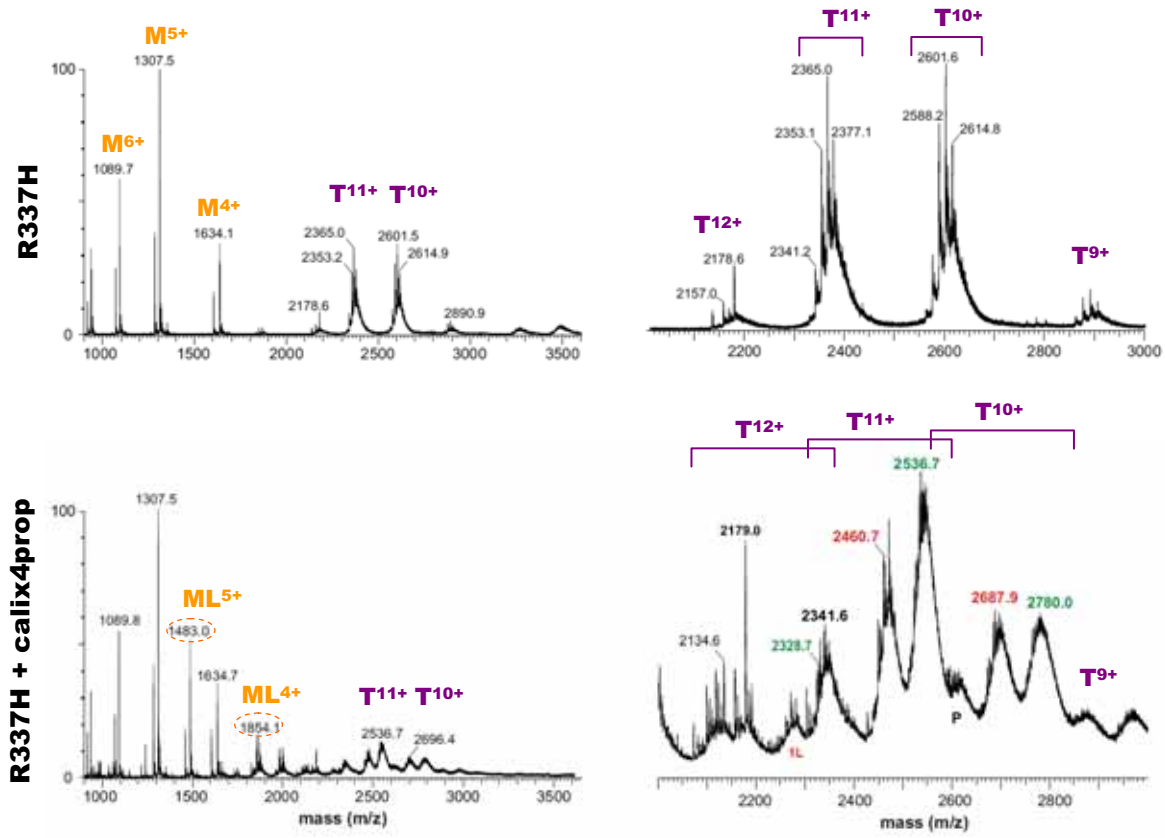

Figure 3.33. ESI-MS spectra of 50μM (monomer) R337H in the presence of 130μM calix4prop in 10mM ammonium acetate buffer pH 7. **T**: tetramer, **M**: monomer, **L**: ligand.

3.6.3. Crystallography: initial trials

Experimental evidence suggested that the strong binding between calix4prop and p53TD promoted significant structural rearrangements (at least) in the protein. Unfortunately, from the available data, little could be established about the actual structure of the complex. Determining the structure would be of utmost importance, since it would help in understanding the molecular recognition event and what makes the complex more stable than the wild-type protein structure; hence, crystallography was selected as an alternative for the structural characterization, although it is not always feasible or easy to achieve the crystallization of a protein-ligand complex.

Below are summarized the results from some preliminary trials. Both soaking and co-crystallization strategies were followed.[48,49]

Soaking p53TD pre-formed crystals into a solution containing calix4prop seriously damaged the well-defined crystals, regardless of the morphology or the buffer used (**Figure 3.34**). The damage was detected after a few hours, although low concentrations of ligand were used, and it was insoluble in the highly saline buffers.

One of the soaked, damaged crystals was diffracted but, as expected, its quality was insufficient for use in characterization. The observed macroscopic effects of calix4prop on protein crystals agreed with the hypothesized protein structural rearrangements upon their tight interaction.

Co-crystallization also was tried. The starting buffers were those already used to crystallize the wild-type protein,[50,51] but calix4prop usually precipitated under those conditions. Amorphous little crystals were detected in some drops; they appeared to correspond to protein, although these crystals have not been analyzed yet (and they might be salts).

Further experiments remain to be done.

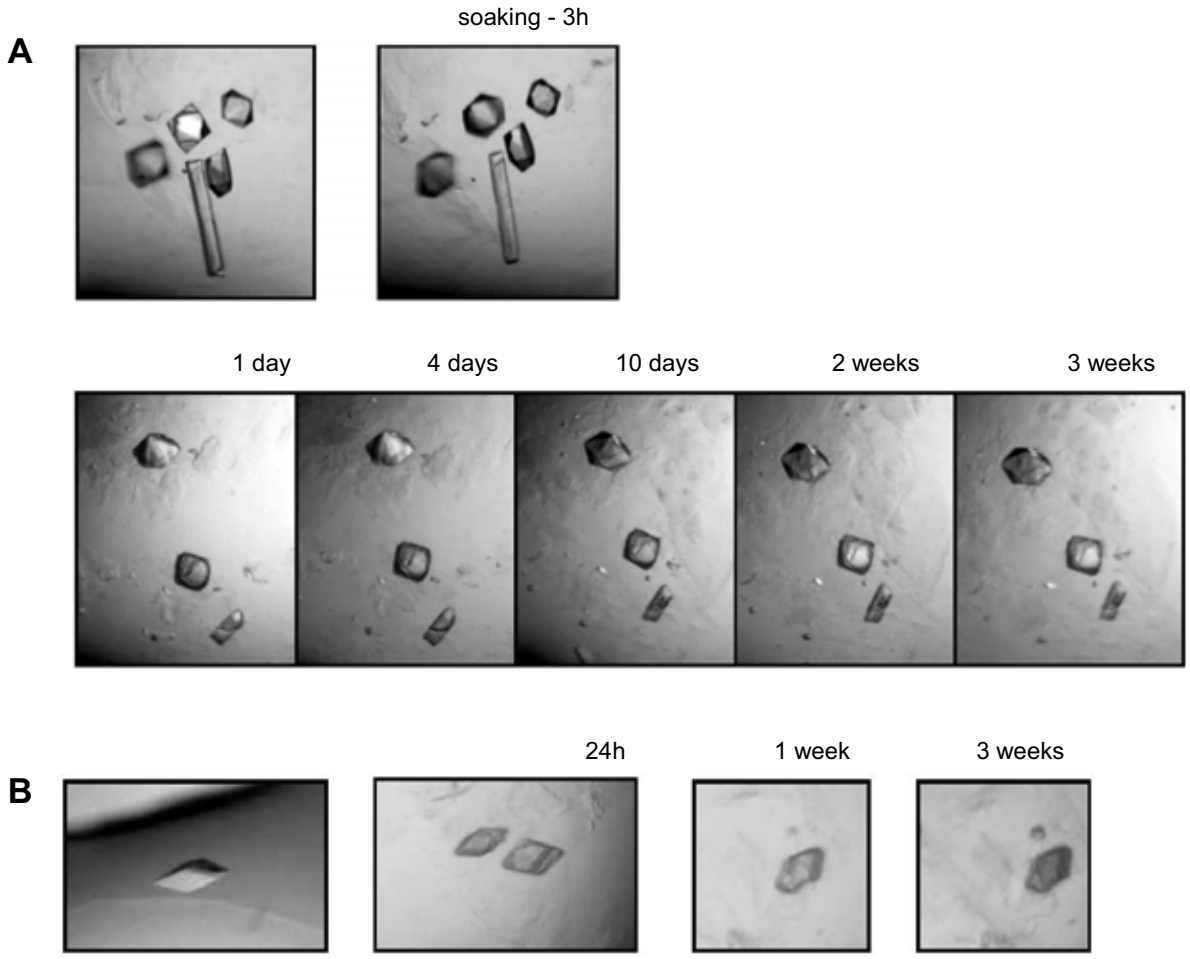

Figure 3.34. Time evolution of p53TD crystals soaked in a solution containing 1.5mM calix4prop, with different crystallization buffers: **(A)** 50mM Tris pH 7.5, 4M sodium formiate, 50mM ammonium sulfate[50] and **(B)** 100mM HEPES pH 7.0, 1M sodium citrate.[51] The unlabelled pictures correspond to the (initial) perfectly defined native crystals, which were damaged in the presence of the ligand.

3.7. Calix4prop overviewed

In the scenario of protein-ligand interactions, entropy has been traditionally considered as a penalty factor, since binding implies loss of freedom for both partners.[52] But the protein and the ligand are not the only players in the interaction; water is also involved. The release of water molecules initially surrounding the individual components to the bulk solvent can counteract the loss of freedom of the interacting partners. Not only the burial of hydrophobic surfaces is counting on that; the pairing of a charge or the removal of a polar group from the exposed surface can have even greater contribution.[53] Nevertheless, the ultimate director of the interaction is the free energy change, for which enthalpy also works. Taken together, it is usually hard to predict beforehand what the net result of an interaction would be like. Calix4prop is a clear example.

Calix4prop is a *para*-guanidinomethyl-calix[4]arene molecule with four flexible propyl chains hanging from the lower-rim. Differing from calix4bridge, the conformation of the calixarene platform is not fixed, although it is still conical. This ligand was designed in order to gain deeper insights onto the role of entropy in the molecular recognition event. Would the entropic penalty from ordering the four flexible propyl chains be too high as to tidily pack them into the hydrophobic pocket of the protein? Could water rearrangements and the hydrophobic interactions overcome that negative factor?

Before performing any experiment, it was naively thought than the entropic penalties would be too high and calix4prop would not interact with the protein. However, the experimental study between the synthetic calix4prop and the tetramerization domains of p53wt, R337H and G334V has revealed that not only they interact, but that calix4prop tightly and specifically binds to the proteins. This underscores the contributions of the hydrophobic effect and of water entropy in molecular recognition processes.

Calix4prop promotes large thermal stabilization in proteins p53wt and R337H; this effect is specific, as proven by the reproduction of the results at two substantially different concentrations (by CD and DSC). The large shift in the melting temperature and the enthalpic increase in the unfolding of the ligand-bound protein suggest a tight and energetic interaction, although whether the ligand dissociates before or during the protein unfolding can not be determined. Interestingly, the calix4prop-complexes of both p53wt and R337H display similar unfolding profiles. Those profiles agree with the simultaneous dissociation and unfolding of a tetrameric species. Indeed, this tetrameric assembly bound to two molecules of ligand is detected by ESI-MS.

The NMR results on the protein also agree with the tight binding of two molecules of calix4prop. The interaction is sequential and –apparently– positively-cooperative. The changes experienced by protein resonances strongly suggest important structural rearrangements upon ligand binding, which would justify the sequential binding, the slow exchange regime and why the less packed R337H is more sensitive.

It is not possible to reliably map the protein binding site based on the changes promoted by calix4prop. Evaluation of a lower affinity calix4prop analog with four amino groups instead of the four guanidinium ones shows that the hydrophobic exposed pocket and the inner hydrophobic core of the protein are the most sensitive regions to the presence of the ligand. This would suggest a hypothetical mechanism in which calix4prop would interact “deep inside” the hydrophobic pocket, somehow “accommodating” its non-polar propyl chains into the non-polar core of the protein.

It is hard to imagine the “disruption” of the stable hydrophobic core of p53TD, which is the actual driven force of tetramerization.[6] If a stable interaction is broken, then a more stable one has to be established. In this case, the loss of freedom in the protein-ligand complex, the disruption of the protein hydrophobic core and its associated structural penalties seem to be definitely over-balanced by the new –tight– hydrophobic and electrostatic interactions established between the protein and the ligand, together with the resulting release of shielding water molecules into the bulk solvent; this is reflected in the high enthalpies detected by DSC and ITC.

The destruction of protein crystals when they are soaked in a calix4prop solution, in conjunction with the changes detected in the CD spectra –likely indicating the disruption of the helix bundle– and the changes in the band pattern of cross-linked protein samples in the presence of calix4prop, would further support the hypothetical mechanism with large structural rearrangements.

From the perspective of the driving forces of the interaction, as previously mentioned, the guanidinomethyl anchoring groups in the upper rim of the calixarene are essential for the tight binding, as well as for the promotion of structural changes. Nevertheless, the hydrophobic component plays the main role in the binding; otherwise the new structure of the complex would not be so stabilized.

By ESI-MS the ligand-bounded complex of p53wt is hardly detected, suggesting the importance of the hydrophobic component. On the contrary, the main species detected for R337H are the tetramer bound to one and to two ligand molecules. This does not mean that hydrophobic interactions are not important for the R337H complex, but electrostatic interactions also contribute to stabilize the complex in the gas-phase. A hypothesis is that the guanidinium-carboxilate chelation of mutant R337H with calix4prop might be better established than for p53wt, probably due to the more optimal binding site that the mutant can arrange. However, for the same reason, the hydrophobic component should also be more important for R337H than for the other.

Regrettably, no information about the binding mode of the ligand has been achieved yet, which prevents us from making any additional hypotheses on the binding mechanisms. Determining the actual ligand binding mode would be invaluable for further understanding the processes implied in the stabilization of the complex. Unfortunately, the tight interaction (actually, the slow chemical exchange) does not allow ready NMR characterization.

For mutant G334V, at room temperature, the changes detected in the structure are the same than those described for p53wt, although it seems to display slightly lesser affinity (as shown by NMR and ITC); this is probably due to its laxer conformation. The surprisingly different behavior of this mutant comes to light when the complex is heated. Within minutes, the tetramerization domain of

mutant G334V undergoes a conformational transformation towards a β-structure which then seems to aggregate into structures whose CD profile resembles that of an amyloid aggregate. This process is specific to this mutant, and the structural mechanisms through which calix4prop prompts the change remain undetermined.

Mutant L344P has served as a non-interacting negative control, thereby proving the specificity of all the molecular recognition processes described for calix4prop, for both the specific binding to the proteins at room temperature and the β-amylodogenesis for G334V at high temperatures.

Therefore, calix4prop certainly interacts with the tetramerization domain of protein p53 and its structured mutants. Regardless of the high thermal stabilization promoted on the tetrameric assembly of p53wt and R337H, the interaction with calix4prop seems to markedly alter the native conformation of the protein. Hence, calix4bridge would best be described as a *"tetramerization stabilizer"* (only for p53wt and R337H). Differing from calix4bridge, calix4prop seems to stabilize a "different" conformation of the tetramer.

Finally, and regarding the questions that arose early on, the importance of flexibility in protein-ligand molecular recognition events has once again been proven. The loss of degrees of freedom upon interaction of the partners, even if it implies strong structural ordering, can definitely be overcome by many other factors, among which the hydrophobic effect is worth mentioning. The tight non-polar interactions established between hydrophobic groups, together with the release of shielding water molecules (that orderly surround those moieties in the free species), can be enough favorable as to promote changes as spectacular as the conformational change of an already stable protein structure (*i.e.* p53wt). In analogy with the positive role of protein flexibility (*i.e.* R337H presents higher affinity presumably because its less packed tetrameric structure enables it to adopt a more optimal conformation), ligand flexibility would also help in setting the optimal conformation to establish the best interactions (differing from calix4bridge whose conformation was rather fixed).

In conclusion, in the challenging design of molecules for protein recognition, flexibility should not be considered as a penalizing factor, but rather the opposite. Molecules in solution are not the fixed structures that we visualize on a computer screen. Although new computational tools to better assess protein internal motions are developed every day, we are still far from being able to predict what actually occurs in solution; indeed, unexpected behaviors are too often observed. Therefore, efficient and accurate ways to deal with flexibility in molecular recognition remain in demand.

Bibliography

1. Chang, C. E., Chen, W. & Gilson, M. K. Ligand configurational entropy and protein binding. *Proc. Natl. Acad. Sci. U. S. A* **104**, 1534-1539 (2007).
2. Yin, F., Cao, R., Goddard, A., Zhang, Y. & Oldfield, E. Enthalpy versus entropy-driven binding of bisphosphonates to farnesyl diphosphate synthase. *J. Am. Chem. Soc.* **128**, 3524-3525 (2006).
3. Fukada, H., Sturtevant, J. M. & Quiocho, F. A. Thermodynamics of the binding of L-arabinose and of D-galactose to the L-arabinose-binding protein of Escherichia coli. *Journal of Biological Chemistry* **258**, 13193-13198 (1983).
4. Manly, S. P., Matthews, K. S. & Sturtevant, J. M. Thermal denaturation of the core protein of lac repressor. *Biochemistry* **24**, 3842-3846 (1985).
5. Waldron, T. T. & Murphy, K. P. Stabilization of proteins by ligand binding: application to drug screening and determination of unfolding energetics. *Biochemistry* **42**, 5058-5064 (2003).
6. Johnson, C. R., Morin, P. E., Arrowsmith, C. H. & Freire, E. Thermodynamic analysis of the structural stability of the tetrameric oligomerization domain of p53 tumor suppressor. *Biochemistry* **34**, 5309-5316 (1995).
7. Celej, M. S., Dassie, S. A., Freire, E., Bianconi, M. L. & Fidelio, G. D. Ligand-induced thermostability in proteins: thermodynamic analysis of ANS-albumin interaction. *Biochim. Biophys. Acta* **1750**, 122-133 (2005).
8. Cooper, A. Heat capacity effects in protein folding and ligand binding: a re-evaluation of the role of water in biomolecular thermodynamics. *Biophys. Chem.* **115**, 89-97 (2005).
9. Mayhood, T. W. & Windsor, W. T. Ligand binding affinity determined by temperature-dependent circular dichroism: cyclin-dependent kinase 2 inhibitors. *Anal. Biochem.* **345**, 187-197 (2005).
10. Privalov, G. P. & Privalov, P. L. Problems and prospects in microcalorimetry of biological macromolecules. *Methods Enzymol.* **323**, 31-62 (2000).
11. Brandts, J. F. & Lin, L. N. Study of strong to ultratight protein interactions using differential scanning calorimetry. *Biochemistry* **29**, 6927-6940 (1990).
12. Shrake, A. & Ross, P. D. Ligand-induced biphasic protein denaturation. *J. Biol. Chem.* **265**, 5055-5059 (1990).
13. Sanchez-Ruiz, J. M. Ligand effects on protein thermodynamic stability. *Biophys. Chem.* **126**, 43-49 (2007).
14. Vuilleumier, S., Sancho, J., Loewenthal, R. & Fersht, A. R. Circular dichroism studies of barnase and its mutants: characterization of the contribution of aromatic side chains. *Biochemistry* **32**, 10303-10313 (1993).
15. Andrew, C. D. *et al.* Stabilizing interactions between aromatic and basic side chains in alpha-helical peptides and proteins. Tyrosine effects on helix circular dichroism. *J. Am. Chem. Soc.* **124**, 12706-12714 (2002).
16. Greenfield, N. J. Applications of circular dichroism in protein and peptide analysis. *TrAC Trends in Analytical Chemistry* **18**, 236-244 (1999).
17. Straus, J. H., Gordon, A. S. & Wallach, D. F. The influence of tertiary structure upon the optical activity of three globular proteins: myoglobin, hemoglobin and lysozyme. *Eur. J. Biochem.* **11**, 201-212 (1969).
18. Lau, S. Y., Taneja, A. K. & Hodges, R. S. Synthesis of a model protein of defined secondary and quaternary structure. Effect of chain length on the stabilization and formation of two-stranded alpha-helical coiled-coils. *J. Biol. Chem.* **259**, 13253-13261 (1984).
19. Manning, M. C. & Woody, R. W. Theoretical determination of the CD of proteins containing closely packed antiparallel beta-sheets. *Biopolymers* **26**, 1731-1752 (1987).
20. Chen, K., Maley, J. & Yu, P. H. Potential inplications of endogenous aldehydes in beta-amyloid misfolding, oligomerization and fibrillogenesis. *J. Neurochem.* **99**, 1413-1424 (2006).
21. Nichols, M. R., Moss, M. A., Reed, D. K., Hoh, J. H. & Rosenberry, T. L. Amyloid-beta aggregates formed at polar-nonpolar interfaces differ from amyloid-beta protofibrils produced in aqueous buffers. *Microsc. Res. Tech.* **67**, 164-174 (2005).
22. Fezoui, Y. & Teplow, D. B. Kinetic studies of amyloid beta-protein fibril assembly. Differential effects of alpha-helix stabilization. *J. Biol. Chem.* **277**, 36948-36954 (2002).
23. Lee, A. S. *et al.* Reversible amyloid formation by the p53 tetramerization domain and a cancer-associated mutant. *J. Mol. Biol.* **327**, 699-709 (2003).
24. Higashimoto, Y. *et al.* Unfolding, aggregation, and amyloid formation by the tetramerization domain from mutant p53 associated with lung cancer. *Biochemistry* **45**, 1608-1619 (2006).
25. Feeney, J., Batchelor, J. G., Albrand, J. P. & Roberts, G. C. K. The effects of intermediate exchange processes on the estimation of equilibrium constants by NMR. *J. Magn Reson.* **33**, 519-529 (1979).
26. Schreiber, G. Kinetic studies of protein-protein interactions. *Curr. Opin. Struct. Biol.* **12**, 41-47 (2002).
27. Pellecchia, M. *et al.* Structural insights into substrate binding by the molecular chaperone DnaK. *Nat. Struct. Biol.* **7**, 298-303 (2000).
28. Johnson, P. E. *et al.* Calcium binding by the N-terminal cellulose-binding domain from Cellulomonas fimi beta-1,4-glucanase CenC. *Biochemistry* **37**, 12772-12781 (1998).
29. Hensmann, M. *et al.* Phosphopeptide binding to the N-terminal SH2 domain of the p85 alpha subunit of PI 3'-kinase: a heteronuclear NMR study. *Protein Sci.* **3**, 1020-1030 (1994).
30. Gunther, U., Mittag, T. & Schaffhausen, B. Probing Src homology 2 domain ligand interactions by differential line broadening. *Biochemistry* **41**, 11658-11669 (2002).
31. Gunther, U. L. & Schaffhausen, B. NMRKIN: simulating line shapes from two-dimensional spectra of proteins upon ligand binding. *J. Biomol. NMR* **22**, 201-209 (2002).
32. Mittag, T., Schaffhausen, B. & Gunther, U. L. Tracing kinetic intermediates during ligand binding. *J. Am. Chem. Soc.* **126**, 9017-9023 (2004).

33. Dudic, M. *et al.* A general synthesis of water soluble upper rim calix[n]arene guanidinium derivatives which bind to plasmid DNA. *Tetrahedron* **60**, 11613-11618 (2004).
34. Nishihara, M. *et al.* Arginine magic with new counterions up the sleeve. *Org. Biomol. Chem.* **3**, 1659-1669 (2005).
35. Sakai, N. & Matile, S. Anion-mediated transfer of polyarginine across liquid and bilayer membranes. *J. Am. Chem. Soc.* **125**, 14348-14356 (2003).
36. Hinshelwood, J. & Perkins, S. J. Conformational changes during the assembly of factor B from its domains by (1)H NMR spectroscopy and molecular modelling: their relevance to the regulation of factor B activity. *J. Mol. Biol.* **301**, 1267-1285 (2000).
37. Hoyt, D. W., Harkins, R. N., Debanne, M. T., O'Connor-McCourt, M. & Sykes, B. D. Interaction of transforming growth factor alpha with the epidermal growth factor receptor: binding kinetics and differential mobility within the bound TGF-alpha. *Biochemistry* **33**, 15283-15292 (1994).
38. Perkins, S. J. & Wuthrich, K. Conformational transition from trypsinogen to trypsin: 1H nuclear magnetic resonance at 360 MHz and ring current calculations. *Journal of Molecular Biology* **138**, 43-64 (1980).
39. Kover, K. E., Groves, P., Jimenez-Barbero, J. & Batta, G. Molecular recognition and screening using a 15N group selective STD NMR method. *J. Am. Chem. Soc.* **129**, 11579-11582 (2007).
40. Post, C. B. Exchange-transferred NOE spectroscopy and bound ligand structure determination. *Curr. Opin. Struct. Biol.* **13**, 581-588 (2003).
41. Ni, F. & Scheraga, H. A. Use of the Transferred Nuclear Overhauser Effect To Determine the Conformations of Ligands Bound to Proteins. *Accounts of Chemical Research* **27**, 257-264 (1994).
42. Ravindranathan, S., Mallet, J. M., Sinay, P. & Bodenhausen, G. Transferred cross-relaxation and cross-correlation in NMR: effects of intermediate exchange on the determination of the conformation of bound ligands. *J. Magn Reson.* **163**, 199-207 (2003).
43. Meyer, B. & Peters, T. NMR spectroscopy techniques for screening and identifying ligand binding to protein receptors. *Angew. Chem. Int. Ed Engl.* **42**, 864-890 (2003).
44. Ladbury, J. E. & Doyle, M. L. *Biocalorimetry 2. Applications of calorimetry in the biological science*. Wiley, West Sussex (2004).
45. Freyer, M. W. *et al.* Binding of netropsin to several DNA constructs: evidence for at least two different 1:1 complexes formed from an -AATT-containing ds-DNA construct and a single minor groove binding ligand. *Biophys. Chem.* **126**, 186-196 (2007).
46. Birnbaum, D. T., Dodd, S. W., Saxberg, B. E., Varshavsky, A. D. & Beals, J. M. Hierarchical modeling of phenolic ligand binding to 2Zn--insulin hexamers. *Biochemistry* **35**, 5366-5378 (1996).
47. Robinson, C. V. *et al.* Probing the Nature of Noncovalent Interactions by Mass Spectrometry. A Study of Protein-CoA Ligand Binding and Assembly. *Journal of the American Chemical Society* **118**, 8646-8653 (1996).
48. Hassell, A. M. *et al.* Crystallization of protein-ligand complexes. *Acta Crystallogr. D. Biol. Crystallogr.* **63**, 72-79 (2007).
49. McNae, I. W. *et al.* Studying protein-ligand interactions using protein crystallography. *Crystallography Reviews* **11**, 61-71 (/1).
50. Jeffrey, P. D., Gorina, S. & Pavletich, N. P. Crystal structure of the tetramerization domain of the p53 tumor suppressor at 1.7 angstroms. *Science* **267**, 1498-1502 (1995).
51. Mittl, P. R., Chene, P. & Grutter, M. G. Crystallization and structure solution of p53 (residues 326-356) by molecular replacement using an NMR model as template. *Acta Crystallogr. D. Biol. Crystallogr.* **54**, 86-89 (1998).
52. Chang, C. E., Chen, W. & Gilson, M. K. Ligand configurational entropy and protein binding. *Proc. Natl. Acad. Sci. U. S. A* **104**, 1534-1539 (2007).
53. Chalikian, T. V. Hydrophobic tendencies of polar groups as a major force in molecular recognition. *Biopolymers* **70**, 492-496 (2003).